ANKARA YILDIRIM BEYAZIT UNIVERSITY

GRADUATE SCHOOL OF NATURAL AND APPLIED SCIENCES



DETECTING MICROWAVE AND MILLIMETER WAVE/THz SIGNALS USING AC DRIVEN GLOW DISCHARGE DETECTORS

M.Sc. Thesis by

HUSSEIN SSALI

Department of Electrical and Electronics Engineering

June 2019

ANKARA

DETECTING MICROWAVE AND MILLIMETER WAVE/THz SIGNALS USING AC DRIVEN GLOW DISCHARGE DETECTORS

A Thesis Submitted to

The Graduate School of Natural and Applied Sciences of

Ankara Yıldırım Beyazıt University

In Partial Fulfilment of the Requirements for the Degree of Master of Science in Electrical and Electronics Engineering, Department of Electrical and Electronics Engineering

By

HUSSEIN SSALI

June 2019

ANKARA

M.Sc. THESIS EXAMINATION RESULT FORM

We have read the thesis entitled **"DETECTING MICROWAVE AND MILLIMTER WAVE/THz SIGNALS USING AC DRIVEN GLOW DISCHARGE DETECTORS"** completed by **HUSSEIN SSALI** under the supervision of **Assoc. Prof. Dr. Asaf Behzat Şahin** and we certify that in our opinion it is fully adequate, in scope and in quality, as a thesis for the degree of Master of Science.

Assoc. Prof. Dr. Asaf Behzat ŞAHİN

(Supervisor)

Prof. Dr. Hüseyin CANBOLAT

(Jury member)

Prof. Dr. Hakan ALTAN

(Jury Member)

Prof. Dr. Ergün ERASLAN

(Director)

Graduate School of Natural and Applied Sciences

ETHICAL DECLARATION

I hereby declare that, in this thesis which has been prepared in accordance with the Thesis Writing Manual of Graduate School of Natural and Applied Sciences,

- All data, information and documents are obtained in the framework of academic and ethical rules,
- All information, documents and assessments are presented in accordance with scientific ethics and morals,
- All the materials that have been utilised are fully cited and referenced,
- No change has been made of the utilised materials,
- All the works presented are original,

and in any contrary case of above statements, I accept to renounce all my legal rights.

2019, June **Hussein SSALI**

ACKNOWLEDGEMENT

I thank the Almighty for enabling me to accomplish this piece of work. I express my earnest appreciation to my supervisor Asst. Prof. Dr. Asaf Behzat Şahin for his guidance, mentoring and selfless support throughout my research. May the Almighty reward him abundantly. I also thank my friends specially Emre Çerçi and Ziaoulrahman Sediqi who have altruistically helped me during my research. I must express my heartfelt gratitude to my family for always supporting me. I am profoundly grateful to all those who have contributed to my academic success in anyway. THANK YOU ALL.

2019, June **Hussein SSALI**

DETECTING MICROWAVE AND MILLIMETER WAVE/THz SIGNALS USING AC DRIVEN GLOW DISCHARGE DETECTORS

ABSTRACT

The use of neon indictor lamp glow discharge detectors (GDDs) has a relatively great potential for a number of microwave and THz detecting and imaging applications. This is so because of their many advantages which include but not limited to; low cost, fast response time and wider dynamic range. In this thesis, we experimentally examine the performance of an AC driven GDD while detecting a THz signal of 60GHz modulated at 170kHz as well as a microwave signal of 10.5GHz. It is observed that driving the GDD with alternating voltage curbs the problem of GDD burn-out that's associated with DC driven GDDs. Nonetheless it is also experimentally proved that the GDD responsivity of a DC driven GDD diminishes with time whereby within 10 minutes the responsivity drops from 100mV to 42mV.

Furthermore, microwave interaction with an AC driven GDD is also examined in that the effect of the distance between signal source of 10.5GHz and the GDD on the signal peak to peak voltage (Vpp) for peculiar modulation frequencies is analyzed. The most efficient modulation frequency is found to be 200kHz followed by 250kHz.

Key words: Terahertz radiation, Microwave, Glow Discharge, Neon indictor lamps, Detection, Plasma

AC TAHRİKLİ GLOW DISCHARGE DETEKTÖRLERİ KULLANARAK MİKRODALGA VE MİLİMETRE DALGA/THZ SİNYALLERİN BELİRLENMESİ

ÖZ

Neon gösterge lambası yanma deşarj dedektörlerinin (GDD'ler) kullanımı, bir dizi mikrodalga ve THz tespit ve görüntüleme uygulaması için nispeten büyük bir potansiyele sahiptir. Bunun nedeni, bunlarla sınırlı olmamak üzere birçok avantajı nedeniyle; Düşük maliyetli, hızlı tepki süresi ve daha geniş dinamik aralık. Bu tez çalışmasında AC tahrikli GDD'nin performansını deneysel olarak incelerken, 170kHz'de modüle edilmiş 60GHz THZ sinyalini ve 10.5GHz'lik bir mikrodalga sinyalini tespit ettik. GDD'yi alternatif voltajla kullanmanın, DC tahrikli GDD'lerle ilişkili GDD yanması sorununu azaltmaya yardımcı olduğu görülmektedir. Bununla birlikte, deneysel olarak, bir DC tahrikli GDD'nin GDD duyarlılığının zamanla azaldığı ve böylece 10 dakika içinde 100 mV'den 42 mV'ye düşen bir duyarlılığın azaldığı kanıtlanmıştır.

Ayrıca, AC tahrikli bir GDD ile mikrodalga etkileşimi de, 10.5GHz sinyal kaynağı ile GDD arasındaki mesafenin, tuhaf modülasyon frekansları için sinyal tepe-tepe voltajı (Vpp) üzerindeki etkisinin analiz edilmesinde incelenmiştir. En verimli modülasyon frekansının 200kHz, ardından 250kHz olduğu bulunmuştur.

Anahtar kelimeler: Terahertz radyasyonu, Mikrodalga, Glow Discharge, Neon gösterge lambaları, Algılama, Plazma

CONTENTS

M.Sc. THESIS EXAMINATION RESULT FORM ii
ETHICAL DECLARATION iii
ACKNOWLEDGEMENT iv
ABSTRACT v
ÖZ vi
CONTENTS vii
ABBREVIATIONS ix
LIST OF TABLES xi
LIST OF FIGURES xii

CHAPTER 1 - INTRODUCTION 1
1.1 Significance of the research 2
1.2 Motivation 3
1.3 Scope of the research 3
1.4 Objectives of the research 3
1.5 Thesis structure 4

CHAPTER 2 - THEORETICAL BACKGROUND AND LITERATURE REVIEW 5
2.1 Glow discharge 5
2.1.1 Applications of Glow Discharge 5
2.1.2 Types of Glow discharge 7
2.1.3 Electrical conduction in gases 9
2.1.4 The qualitative features of a Glow Discharge 11
2.2 Measurement of the fundamental plasma parameters 14
2.2.1 Electron temperature 14
2.2.2 Electron density 16
2.3 Microwave and Millimeter wave (THz) radiations 16
2.3.1 Microwave radiation 16
2.3.2 Millimeter wave radiation 19
2.4 Microwave and Millimeter wave interaction with GDDs 19

2.5 A literature review on using neon indicator lamps for detecting microwave and millimeter wave signals 22

CHAPTER 3 - METHODOLOGY 29

3.1 Research Methodology 29

3.2 Experimental setup 30

3.2.1 Millimeter wave/THz detection 30

3.2.2 Microwave detection. 34

CHAPTER 4 - RESULTS 36

4.1 THz Detection 36

4.1.1 Signal modulation 36

4.1.2 Signal detection before filtering 36

4.1.3 Signal detection after first filtering 39

4.1.4 Signal detection after amplification 41

4.1.5 Signal detection after secondary filtering 43

4.2 Responsivity of a DC driven GDD 46

4.3 Effect of the modulation frequency on the detected microwave signal 47

4.4 Effect of the distance between the GDD and the signal source on the detected microwave signal 48

CHAPTER 5 - CONCLUSION 51

5.1 FUTURE WORK 51

REFERENCES 52

CURRICULUM VITAE 56

ABBREVIATIONS

AC Alternating Current

CW Continuous Wave

DC Direct Current

EM Electro-Magnetic

FPA Focal Plane Array

FWHM Full Width Half Maximum

GDD Glow Discharge Detector

GHz Gigahertz

Hz Hertz

IC Integrated Circuit

IF Intermediate Frequency

kHz Kilohertz

LO Local Oscillator

LTE Local Thermal Equilibrium

MHz Megahertz

mm Millimeter

NEP Noise Equivalent Power

OES Optical Emission Spectroscopy

PLL Phase Lock Loop

PD Potential Difference

RF Radio Frequency

THz Terahertz

VCO Voltage Controlled Oscillator

LIST OF TABLES

TABLE 2.1 CHARACTERISTIC PARAMETERS FOR DC GLOW DISCHARGE 8

TABLE 2.2 MICROWAVE FREQUENCY BANDS AS DESIGNATED BY THE RADIO SOCIETY OF GREAT BRITAIN (RSGB)..... 18

TABLE 4.3 MODULATION FREQUENCIES VERSUS VOLTAGE FOR MICROWAVE 47

TABLE 4.4 EFFECT OF DISTANCE ON 200KHZ AND 250KHZ MODULATION FREQUENCIES 49

LIST OF FIGURES

FIGURE 2.1 CLASSICAL DC ELECTRICAL DISCHARGE TUBE 6
FIGURE 2.2 PARALLEL PLATE PLASMA REACTOR 6
FIGURE 2.3 COAXIAL ELECTRON BOMBARDMENT DISCHARGE CHAMBER 6
FIGURE 2.4 SCHEMATICS OF A DC GLOW DISCHARGE 7
FIGURE 2.5 VOLTAGE-CURRENT CHARACTERISTICS FOR A DC GLOW DISCHARGE. 10
FIGURE 2.6 NORMAL GLOW DISCHARGE CHARACTERISTICS AND THEIR FEATURE PROFILES. 13
FIGURE 2.7 BOLTZMANN'S PLOT TO DETERMINE ELECTRON TEMPERATURE. 15
FIGURE 2.8 THE EM SPECTRUM 17
FIGURE 3.9 RESEARCH METHODOLOGY 29
FIGURE 3.10 THE GDD USED 30
FIGURE 3.11 THE BIASING CIRCUIT 31
FIGURE 3.12 THE FILTER CIRCUIT 32
FIGURE 3.13 THE AMPLIFIER CIRCUIT 33
FIGURE 3.14 THE SCHEMATIC DIAGRAM FOR THE WHOLE SETUP 33
FIGURE 3.15 THE EXPERIMENTAL SETUP 34
FIGURE 3.16 THE MICROWAVE DOPPLER SENSOR USED 35
FIGURE 3.17 GDD USED FOR MICROWAVE DETECTION 35
FIGURE 3.18 THE MICROWAVE DETECTION SCHEMATIC 35
FIGURE 4.19 AC DRIVE VOLTAGE AND RLOAD VOLTAGE WITH THZ OFF 36
FIGURE 4.20 I-V CURVE FOR THE GDD WİTHTHZ OFF 37
FIGURE 4.21 AC DRIVE VOLTAGE AND RLOAD VOLTAGE WITH THZ ON 37
FIGURE 4.22 I-V CURVE FOR THE GDD WITH THZ ON 38
FIGURE 4.23 RECEIVED SIGNAL MAGNITUDE VERSUS I_{GDD} 39
FIGURE 4.24 AC DRIVE VOLTAGE AND RECEIVED FILTERED SIGNAL WITH THE THZ SOURCE OFF 40
FIGURE 4.25 AC DRIVE VOLTAGE AND RECEIVED FILTERED SIGNAL WITH THE THZ SOURCE ON 40
FIGURE 4.26 SIGNAL SPECTRUM OF THE FILTERED SIGNAL WITH THE THZ SOURCE ON 41
FIGURE 4.27 AC DRIVE VOLTAGE AND RECEIVED AMPLIFIED SIGNAL WITH THE THZ SOURCE ON 42
FIGURE 4.28 SIGNAL SPECTRUM OF THE AMPLIFIED SIGNAL 42
FIGURE 4.29 AC DRIVE VOLTAGE AND SECONDARY FILTERED SIGNAL WITH THE THZ SOURCE OFF 43

FIGURE 4.30 SIGNAL SPECTRUM OF THE SECONDARY FILTERED SIGNAL WITH THE THZ SOURCE OFF 43
FIGURE 4.31 AC DRIVE VOLTAGE AND SECONDARY FILTERED SIGNAL WITH THE THZ SOURCE ON . 44
FIGURE 4.32 SIGNAL SPECTRUM OF THE SECONDARY FILTERED SIGNAL WITH THE THZ SOURCE ON 44
FIGURE 4.33 DC SUPPLY NOISE 45
FIGURE 4.34 FFT FOR DC SUPPLY NOISE 45
FIGURE 4.35 RESPONSIVITY DECAY FOR A DC DRIVEN GDD 46
FIGURE 4.36 VPP (MV) VERSUS MODULATION FREQUENCY (KHZ) FOR MICROWAVE 48
FIGURE 4.37 VPP (MV) VERSUS DISTANCE (CM) FOR MICROWAVE 50

CHAPTER 1

INTRODUCTION

The microwave and millimeter (mm) wave/THz regions of the electromagnetic spectrum have become very prominent for applications such as communications, defense, medicine and space technology [1]. Nonetheless, THz imaging systems have also been applied in spectroscopic characterization, packaging and quality control. This has been due to their numerous advantages which include but not limited to; no or insignificant harm to biological tissues and this is because of their low photon energy property, ability to easily penetrate non-polar and nonmetallic materials and low atmospheric scattering as well as turbulence effects as compared to optical rays and infrared.

It is needful to note that there are challenges that exist in the development of improved microwave and THz radiation sources and detection technologies in that there is need for inexpensive and ideally sensitive room temperature detectors in the spectral regions of microwave and THz. Generally, there are three types of room temperature detectors; Pyroelectric detectors, Golay cells and Schottky diodes [2]. A Schottky diode is an exceedingly fast room temperature THz detector with a low noise equivalent power (NEP) of 10^{-10} W/Hz$^{1/2}$ [3]. Ideally, Schottky diodes may be applied for measurements above 1.5 THz, however they are less sensitive and necessitate more local oscillator (LO) power as compared to conventional tunable LO sources [4]. Pyroelectric detectors and Golay cells have a wide spectral response (0.1–10 THz) as well as a low NEP (less than 10^{-10} W/Hz$^{1/2}$), however they have a long response time and a modulation frequency that is limited to a few hertz [2]. It is noteworthy that all these detectors are expensive.

However, the use of novel miniature neon indictor lamp glow discharge detectors (GDDs) bears a relatively outstanding potential for a spate of microwave and THz detecting and imaging applications and have been studied for some time. GDDs have a multitude of advantages which include but not limited to; low cost (less than one dollar), faster response time, electronic ruggedness, wide dynamic range whereby it can hardly be damaged by inadvertent outbursts of

power, broad spectral range whereby one tube can be used in both the microwave and mm wave spectral regions, potential to operate at high temperatures, simple to use and can act as a transducer and a receiving antenna simultaneously. It is posited in [5], that the response time of GDDs is 14–100 ns, their NEP is 10^{-12} W/Hz$^{1/2}$, and their spectral response is from microwave to X-ray.

The detection mechanism normally used in the microwave band is the enhanced cascaded ionization because of the higher electromagnetic wave electric fields. The threshold of the breakdown intensity tends to step-up with EM frequency because there is relatively limited time for electrons to attain kinetic energy that is equal to ionization energy before the electric field can reverse direction. For shorter wavelengths, the gases are broken down by multi-photon ionization and the required threshold for this breakdown decreases as the frequency increases. Thus, for THz and infrared bands the required threshold for gas breakdown is high, and in this region, the GDDs have minimum responsivity. Nevertheless, GDDs are constrained by internal noise which is a salient feature of almost all plasma devices.

1.1 Significance of the research

The research can be a source of literature to the overall research that is being undertaken today due to the continuous need for new technologies with greater capacity, reduced cost as well as improved reliability that need to be employed in detection applications. This is so because the research gives;

- An in-depth theoretical study of glow discharge physics.
- A synopsis on microwave and millimeter wave radiations.
- A thorough exposition as well as an experimental examination of microwave and millimeter wave interaction with AC biased glow discharge detectors (GDDs).
- A comprehensive review of research work done on using neon indicator lamps as GDDs for detecting microwave and millimeter wave signals.

Nonetheless the research also widens and enriches the researcher's knowledge as far as microwave and terahertz signals' applications are concerned thereby promoting the feel for innovativeness and creativity.

1.2 Motivation

Plasma produced by gases renders a distinctive detection forum for electromagnetic (EM) radiations. The fact that its physical and electrical features can be controlled as well as its ease of inception with a low-bias voltage has motivated research in its applications especially detection. In our research, the performance of an alternating current (AC) glow discharge detector while detecting microwave and terahertz radiations is examined and analyzed theoretically and experimentally since prior to the use of any novel concept, in a field where efficiency and safety are paramount, considerations must be comprehensively exposited, and it must be shown that it is compatible with the standard requirements.

1.3 Scope of the research

There is a significant upsurge of research interest in signal detection using glow discharge detectors (GDDs) in pursuit for novel technologies with higher efficiency, improved reliability as well as reduced cost for detection applications. Notably in most of the previous research work, experiments have been carried out using a DC biased GDD in that there is lack of a comprehensive experimental examination of the performance of an AC biased GDD yet driving the GDD with AC offers substantial advantages. Thus, in this thesis we experimentally examine and analyze the performance of an AC driven GDD while detecting microwave and THz signals.

1.4 Objectives of the research

The main objective of the research is to detect microwave and millimeter wave signals using AC driven neon indicator lamp GDDs. Nevertheless, the specific objectives of the research are;

- To design and implement an AC biasing circuit for the GDD.
- To design and implement filters and an amplifier for the detected signal.
- To generate a microwave (X-band) and a millimeter wave signal.
- To comprehensively analyze the detected signal by an AC driven GDD.
- To analyze a DC biased GDD responsivity with respect to time.
- To analyze the effect of the distance between the GDD and the signal source on the peak to peak voltage of a microwave signal for particular modulation frequencies.

1.5 Thesis structure

The thesis is structured in five chapters; chapter one gives an introduction where a precise background information, significance, motivation, scope and objectives of the research are given. Chapter two comprehensively expounds on the theory of glow discharge as well as expositing its types, applications and its interaction with microwave and millimeter wave radiations. Even so, a literature review on using neon lamps for detecting microwave and millimeter wave signals is presented in this chapter. Chapter three gives a detailed account of the experimental setup for our work whereas chapter four discusses findings and analyzes results. Chapter five gives the conclusion and suggestions for future research points.

CHAPTER 2

THEORETICAL BACKGROUND AND LITERATURE REVIEW

2.1 Glow discharge

A glow discharge can be referred to as a plasma that is formed when electric current passes through a gas. In fact, its name reposes on the conception that plasma is luminous because visible light can be generated by excitation, collisions and recombination [6]. It is created when a voltage is applied between two electrodes in a glass-tube with a low-pressure gas. When this voltage surpasses a "striking voltage", the ionization of the gas becomes self-sufficing thereby making the tube glow with a particular color depending on the gas used.

2.1.1 Applications of Glow Discharge

Glow discharges have a great deal of applications. The ability to emit light renders them a spate of applications in the light industry as electrical discharge tubes in fluorescent lamps and neon discharge tubes for adverts, as flat display panels for television screens and as pump sources for gas lasers.

Furthermore, glow discharges have got applications in the material processing technology and micro-electronics industry. These include;

- Etching of surfaces for IC fabrication
- Deposition for thin protective coatings
- Plasma modification for polymers
- Surface treatment
- Plasma polymerization

Other industrial applications include electron bombardment with plasma sources and plasma reactors with DC parallel plates [7] as illustrated in figure *2.1*.

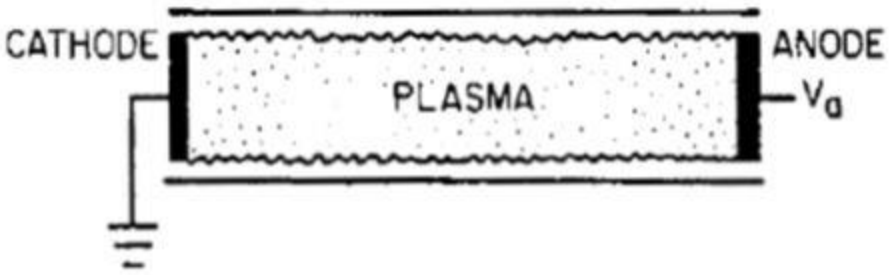


Figure 2.1 Classical DC Electrical Discharge Tube

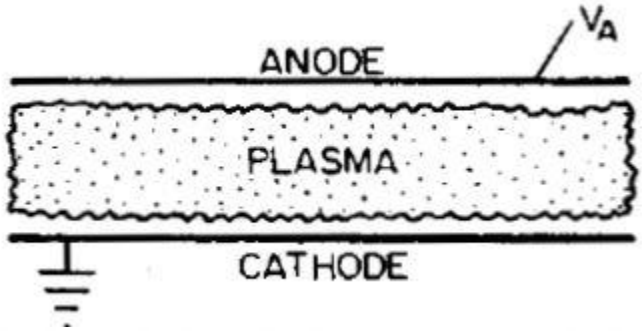


Figure 2.2 Parallel Plate Plasma Reactor

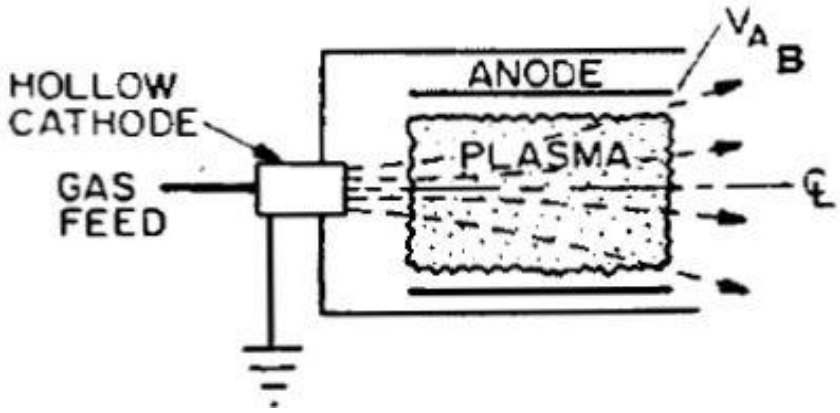


Figure 2.3 Coaxial Electron Bombardment Discharge Chamber

2.1.2 Types of Glow discharge

There are many different types of glow discharge and below is an elucidation of the most common ones;

***Direct current (dc) glow discharge*.** This is formed when a potential difference (pd) is applied between two electrodes which are put in a chamber with a reactive or an inert gas at a given pressure [7] as shown in fig.

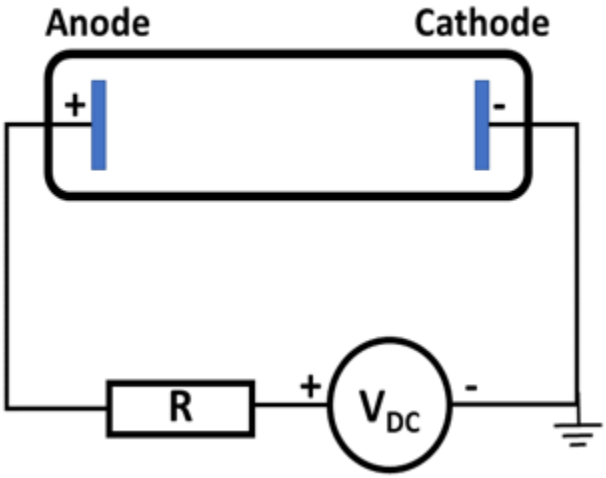


Figure 2.4 Schematics of a dc glow discharge

The applied pd leads to increased collisions with gas atoms and molecules which may lead to ionization and excitation. This creates excited species, which decays to low levels by light emission hence a "glow" discharge. The ions are sped up to the cathode and emit secondary electrons after bombardment on the cathode surface. These electrons are sped up away from the cathode and lead to other ionization collisions. The ionization collisions give rise to ion-electron pairs, and this renders a glow discharge a self-sufficed plasma. A pd is applied continuously between the cathode and anode, giving a constant current.

Table 2.1 Characteristic parameters for DC Glow Discharge

Parameter	**Low Value**	**Characteristic Value**	**High Value**
Neutral gas pressure (Torr)	10^{-6}	0.5	760
Electrode voltage (V)	100	1000	50000
Electrode current (A)	10^{-4}	0.5	20
Number density (electrons/m^3)	10^{14}	5e15	6e18
Electron kinetic temperature (eV)	1	2	5
Power level (W)	10^{-2}	200	250000
Plasma volume (liters)	10^{-6}	0.1	100

Capacitively coupled radio-frequency (ccrf) glow discharge. The dc glow discharge problem maybe overcome using ccrf glow discharge and this is by applying an alternating voltage between electrodes. The charge during one half cycle is neutralized by the opposite charge in the next half-cycle [7]. In this case the role played by the cathode and anode changes alternately. It should be noted that ccrf is a kind of an ac glow discharge.

Noticeably, the electrodes may be covered by a dielectric barrier and this is referred to as the *dielectric barrier discharge (DBD).*

Pulsed glow discharge. The glow discharge can also be operated by a pulsed current source. This kind of glow discharge has short glow discharges in the millisecond or microsecond range, succeeded by an after-glow of a longer period. The pulsed glow discharge has an advantage of

high peak power levels being attainable for low average power levels leading to improved efficiencies.

The magnetron glow discharge. In this type of discharge, a magnetic field is applied hence both magnetic and electric fields prevail. The electrons rotate around the magnetic field lines in helices and create ionization. Thus, they are operated at low pressure and high current as compared to other glow discharges. There are different types of magnetron configurations which include planar, cylindrical, and circular magnetrons.

Several other types of glow discharge with high plasma density and low pressure have been developed. Generally, in these glow discharges, power is applied by electromagnetic induction, not by a potential difference between electrodes. For example, in the *inductively coupled glow discharge*, where power is inductively coupled to the electrodes.

2.1.3 Electrical conduction in gases

Conduction in gases normally needs charge carriers (ions or electrons). The charge carriers arise from ionization of gas molecules. With respect to the flow of current, glow discharge lies between the dark discharge and arc discharge as illustrated in fig.

- In the dark discharge, gas ionization is by a radiation source which can be a microwave or a THz radiation. When a high voltage is applied between the anode and the cathode, the carriers that are free can gain sufficient energy for more carriers to be freed. This process is known as the ***Townsend avalanche***.

- In a glow discharge, a point can be reached when the electrons leaving the cathode permits other electrons to leave the cathode during the process of carrier generation. In this case, the average electron can cause some ionization through the Townsend avalanche and the ensuing positive ions goes to the cathode, and some dislodge other electrons by secondary emission.

- In the arc discharge, electrons withdraw from the cathode by field emission and thermionic emission , and gas ionization is thermal.

Beneath the breakdown voltage, the electric field is constant and little or no glow is realized. The Townsend discharge begins when there is enough electric field for ionization. The electric

field is adjusted by the availability of positive ions when a glow discharge springs up. The glow discharge begins as normally, and more cathode surface is engaged in the glow with increased current. When the current increases beyond the level where the whole cathode surface is engaged, the discharge is an abnormal glow. When the current increases further, an arc discharge starts.

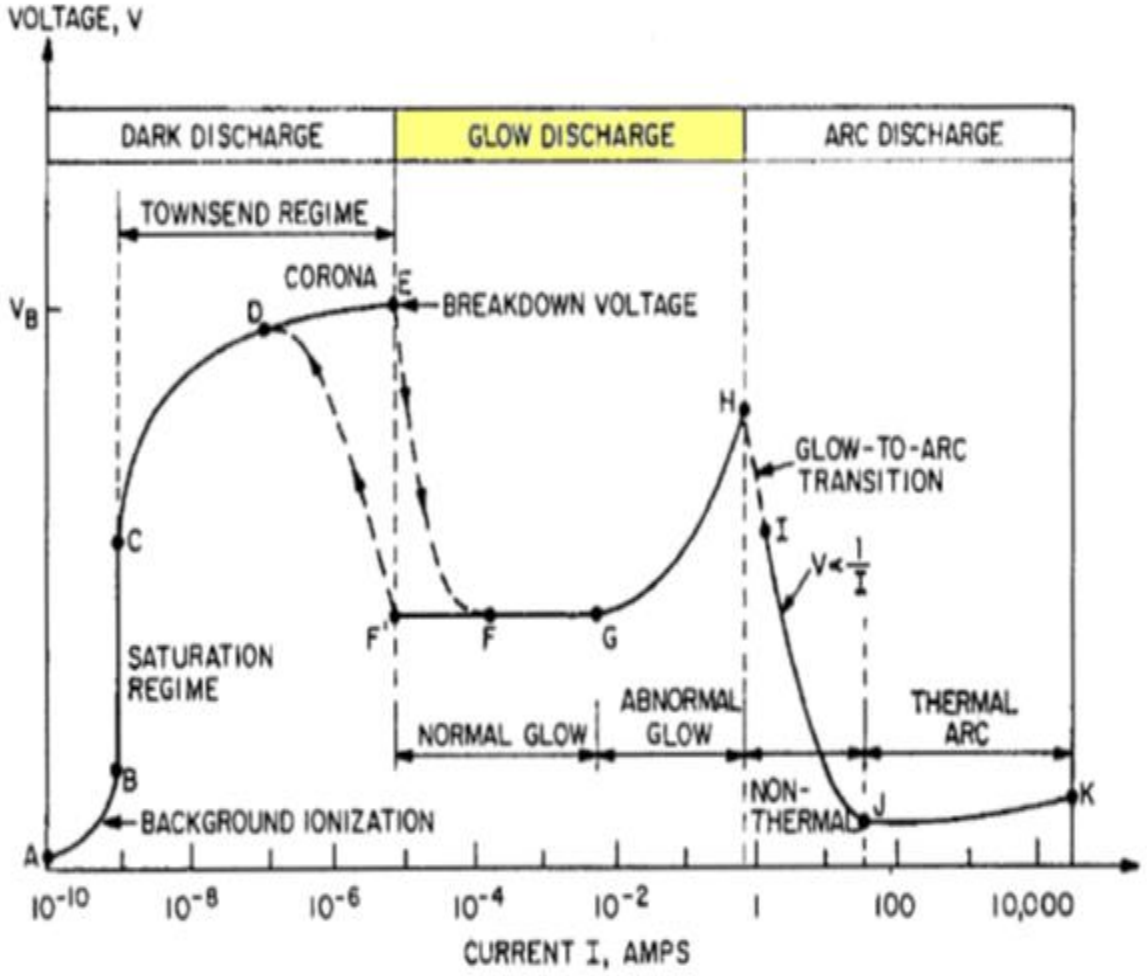


Figure 2.5 Voltage-Current characteristics for a DC glow discharge.

2.1.4 The qualitative features of a Glow Discharge

The characteristics of a glow discharge during normal glow is illustrated in figure 2.6 and below is an explanation of the different regions;

The Cathode

The emission of secondary electrons at the surface of the cathode is important for a self-sufficing glow discharge. When an ion bombards the cathode surface, secondary electrons are emitted. The current density is therefore [6];

$$J = \frac{J_O e^{\alpha d}}{1-\gamma(e^{\alpha d}-1)} \quad A/m^2 \qquad \textbf{(2.1)}$$

Aston dark space

This is the dark region after the cathode. It has space charge that is negative and a stronger electric field. The electrons herein are slow and of low energy and density [6]. In this region, the roaming electrons combined with the electrons from secondary emission outnumber the ions [8].

Cathode glow

This region has a higher ion density and the electrons have enough energy to excite the atoms with collision. Because of the emitted excited atoms, it is sometimes orange or reddish. The gas type and pressure determine its axial length.

Crookes dark space

This region has a relatively moderate electric field and nevertheless voltage drop normally happens here. Its space charge is ideally positive with a higher ion density [9].

Negative glow

The negative glow has the brightest intensity with a lower electric field. It is normally larger than the cathode glow, and the electrons carry almost the entire current in this region. Here the accelerated electrons to the cathode region lead to excitation and ionization, thus the brighter light.

Faraday dark space

The electric field and energy as well as the space charge in this region are relatively low. The density of the electron number reduces by diffusion and recombination.

Positive Column

In this region, the electric field is low (1 V/cm). It is just enough to uphold the necessary extent of ionization at the end of the cathode. The density of the electron number in this region is about 1015 electrons/m^3, with 1 to 2 eV of electron kinetic temperature. The positive column is long, and its length may be adjusted by altering the separation of the electrodes at a uniform voltage drop and pressure. The plasma in the positive column is normally blue or pink.

Anode glow

The anode glow is a bit more intense and it is not always on, despite its brightness. It acts as the edge for the anode sheath [6].

Anode dark space

This is between the anode and the anode glow. It is the sheath of the anode with a space charge that is negative because electrons are traversing to the anode from the positive column. The electric field herein is higher than that in the positive column.

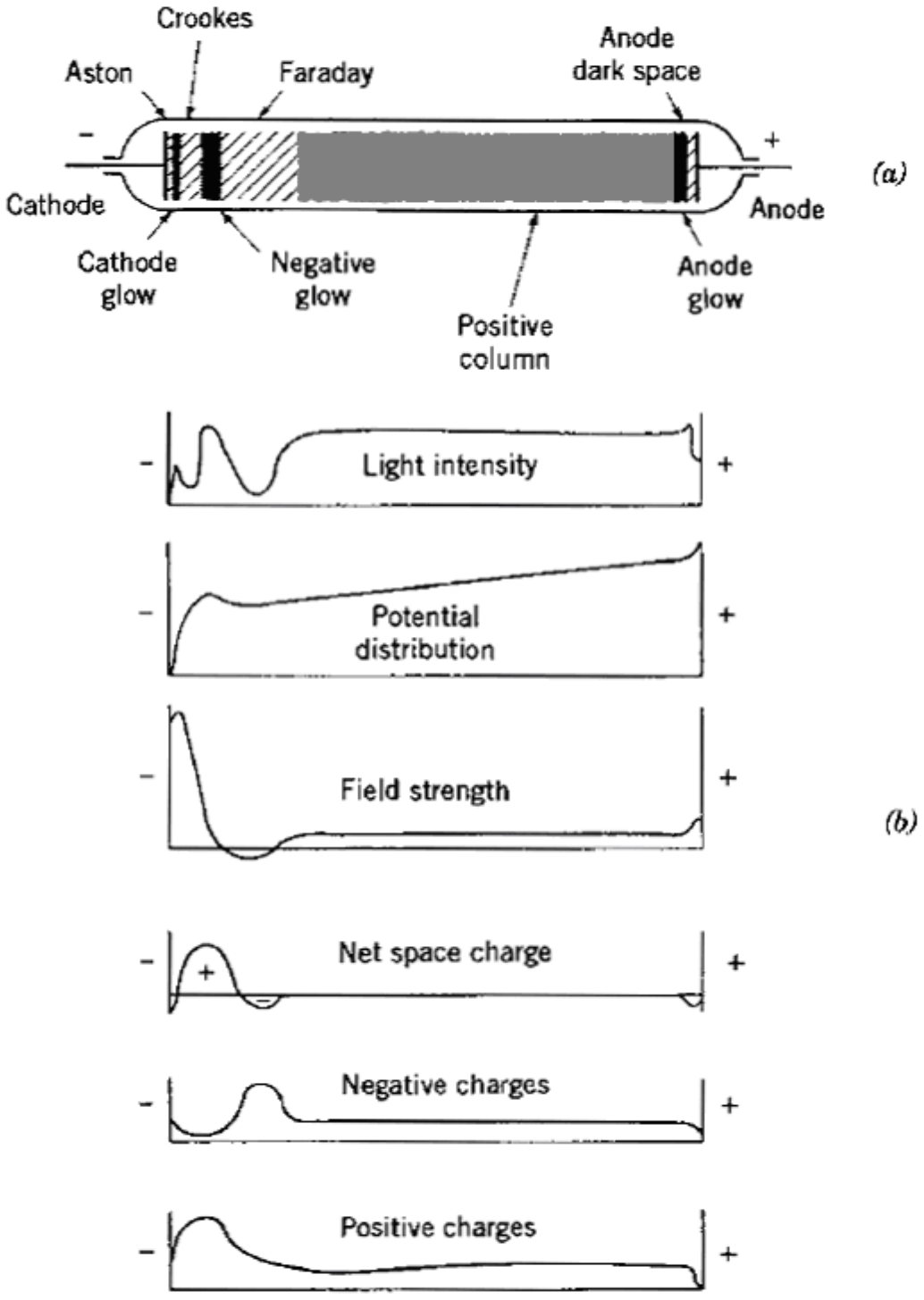


Figure 2.6 Normal glow discharge characteristics and their feature profiles [9].

2.2 Measurement of the fundamental plasma parameters

The most used technic for measuring and analyzing fundamental plasma parameters like the electron density and temperature, is the ***Optical Emission Spectroscopy (OES)*** and this is because of its non-invasive characteristic. When using the OES, the light intensity from plasma is measured with respect to wavelength. Because of the inelastic collisions between electrons, the atom state tends to rise to an electronic state and in the due process, there is a photon emission within a particular wavelength. The emitted photon energy is;

$$E_p - E_q = \frac{hc}{\lambda_{pq}} \quad \textbf{(2.2)}$$

Where E_p and E_q are the upper state energy and lower state energy respectively, the Planck's constant is *h*, *c* is the light speed and λ_{pq} is the operational wavelength [10].

The spectral line intensity because of atom transition from the upper state to the lower state under local thermal equilibrium (LTE) conditions is [11];

$$I_{pq} = \frac{hcA_{pq}g_p n}{\lambda_{pq}U(T)} exp\ (-E_p/k_B T) \quad \textbf{(2.3)}$$

Where A_{pq} is the transition probability, g_p is the upper state statistical weight, *n* is the emitting species number density, *U(T)* is the atom partition function, k_B is the known Boltzmann's constant and T is the temperature of the excitation process.

2.2.1 Electron temperature

Under LTE conditions, the temperature of the electrons is equal to the temperature of the excitation process *(T)* in (2.3) and thus can be determined using the equation. Nevertheless, other methods for temperature measurements are explained below:

The spectral line ratio method

By finding out the spectral intensity lines ratio subscribing to identical atomic kinds, the temperature of an electron can be ascertained. Two dissimilar spectral lines are selected from the emission spectrum and the spectral lines intensities obtained due to a transition from p to q and

m to n are taken to be I_{pq} and I_{mn}, respectively. Using the (2.3), the two spectral lines intensity ratio is;

$$\frac{I_{pq}}{I_{mn}} = \frac{\lambda_{mn} g_p A_{pq}}{\lambda_{pq} g_m A_{mn}} \exp\left(-\frac{E_p - E_m}{k_B T_e}\right) \quad \textbf{(2.4)}$$

The Boltzmann's Plot method

For error reduction, more than two spectral lines belonging to the same atom kinds are used and in this case the Boltzmann's plot is used to ascertain the temperature. Equation (2.3) can be rearranged as;

$$\ln\left[\frac{I_{pq}\lambda_{pq}}{A_{pq} g_p}\right] = -\frac{E_p}{k_B} + \ln\left[\frac{n}{U(T)}\right] \quad \textbf{(2.5)}$$

The equation above gives a linear relationship plot with a $-1/k_B T_e$ slope as illustrated in Figure and the temperature is derived from the determined slope [12].

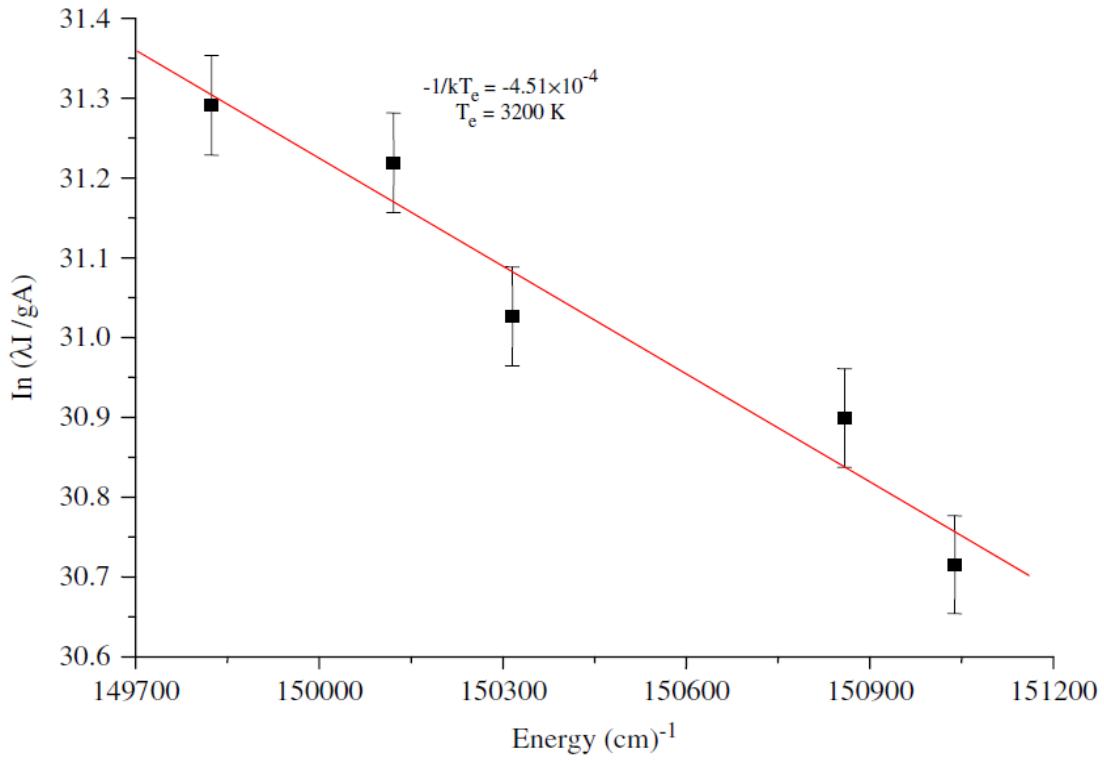


Figure 2.7 Boltzmann's plot to determine electron temperature [12].

2.2.2 Electron density

Plasma can also be characterized by the electron density. In an OES, the spectral lines can be shifted and broadened. Broadening technics include; natural, stark, instrumental and doppler broadening [13]. The Stark broadening is the mostly used technic. Its profile spectral line has a full-width half-maximum (FWHM) correlating to the electron density. The spectral line FWHM is [14];

$$\Delta\lambda_{1/2} = 2\mathrm{w}\left(\frac{N_e}{10^{16}}\right) \quad \textbf{(2.6)}$$

Where w is the parameter of the electron impact and N_e is the electron density.

2.3 Microwave and Millimeter wave (THz) radiations

In this section, we give a synopsis on microwave and millimeter wave (THz) radiations.

2.3.1 Microwave radiation

The electromagnetic radiations are generally assorted into the following bands or regions as illustrated in figure *2.8*;

- Gamma
- X-ray
- Ultraviolet
- Visible
- Infrared
- Terahertz
- Microwave
- Radio waves

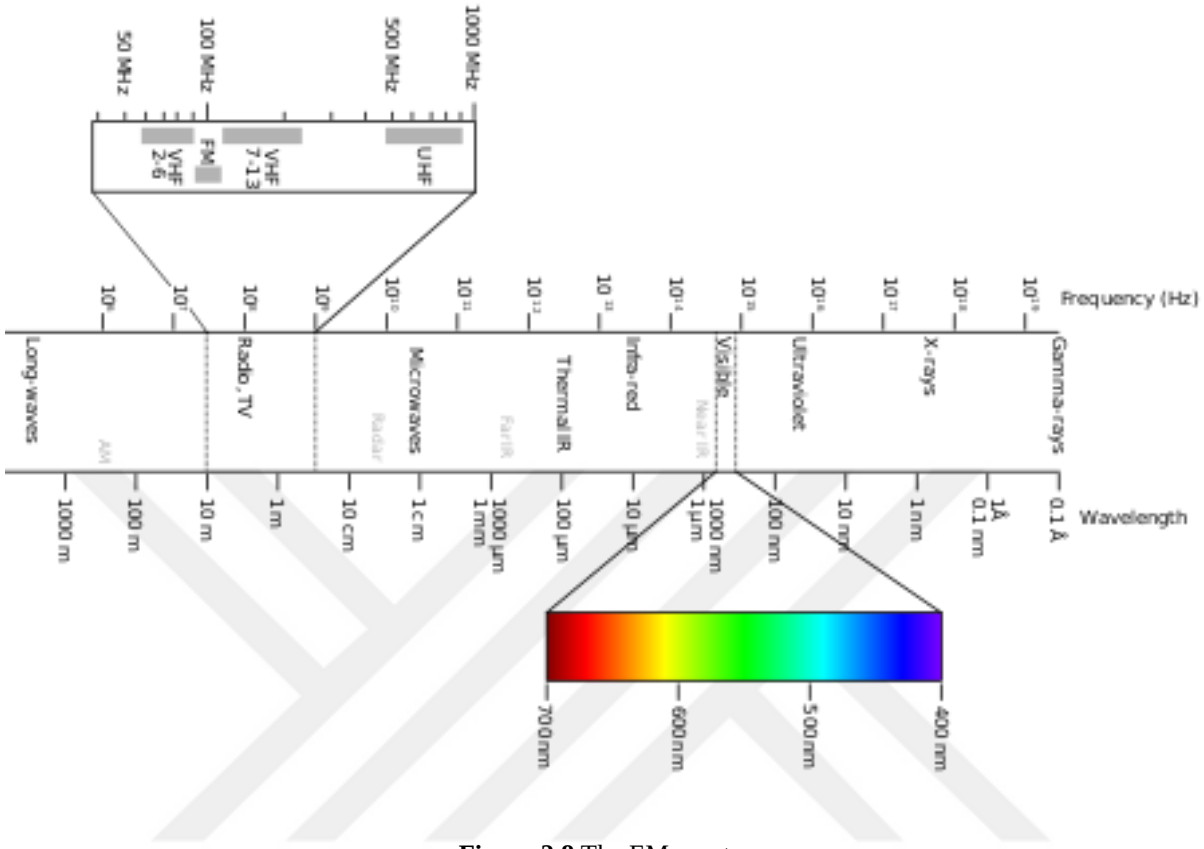


Figure 2.8 The EM spectrum

Microwave radiations have frequencies between 300 MHz and 300 GHz with wavelengths of about 1m to 1mm. Microwave frequencies are oftentimes designated as; L, S, C, X, K_u, K and K_a bands.

2.3.1.1 Microwave sources

Microwave sources can be classified as low-power and high-power microwave sources. Low-power microwave sources normally use solid-state devices like tunnel diodes, field-effect transistors (FETs), and Gunn diodes [37]. These sources can be in formats like; embeddable modules, benchtop instruments, card-level and rackmount instruments. Microwave radiations are usually amplified by a solid-state device known as a maser which has the same working principle as a laser. The high-power microwave sources normally utilize special vacuum tubes for microwave generation. They operate using the principle of ballistic electron motion in a vacuum with controlled electric and magnetic fields. They also include; klystron, magnetron and gyrotron. The working principle of these devices is the ballistic flying of electrons.

2.3.1.2 Microwave applications

The following are some of the microwave applications:

Microwave technology is broadly used for P2P communication since it can allow frequency reuse and has relatively higher frequencies that allow higher data transmission rates because of the wider bandwidth. Microwaves can also be used for spacecraft communication, TV, communication satellites and radar technology. Furthermore, microwave radiations are used in spectroscopy, especially in the X-band region (8-12 GHz).

Table 2.2 Microwave frequency bands as designated by the Radio Society of Great Britain (RSGB).

Designation	**Frequency (GHz)**	**Wavelength**	**Applications**
L band	1 to 2	15 - 30 cm	GPS, GSM, Military telemetry
S band	2 to 4	7.5 - 15 cm	Radar, astronomy, Bluetooth, amateur radio, wireless LAN, ZigBee, microwave ovens
C band	4 to 8	3.75 - 7.5 cm	Long-distance radio communications
X band	8 to 12	25 - 37.5 mm	Radar, satellite, communication, spectroscopy, terrestrial broadband, amateur radio

2.3.2 Millimeter wave radiation

Millimeter wave or Terahertz (THz) radiations are EM waves between 0.3 – 3 THz on the EM spectrum as designated by ITU. Their wavelengths are in the range of 1 mm to 0.1 mm.

2.3.2.1 THz sources

THz radiations have both natural and artificial sources. Naturally, THz radiations are generated as part of the blackbody radiations from anything that has a temperature higher than 2 Kelvins. Whereas artificially, THz radiation sources include; varactor multipliers, the gyrotron, Schottky diode multipliers, the free electron laser (FEL) and far infrared (FIR) laser, photo-mixing sources, pulsed sources applied in THz time-domain spectroscopy, solid-state sources as well as electronic oscillators using resonant tunneling diodes [38].

2.3.2.2 THz applications

THz radiations can be used in a spate of applications which include but not limited to;

- Medical imaging since they do not damage tissues because of their low-photon energies.
- Security and this is because they can easily penetrate plastics and other fabrics.
- Scientific use and imaging like in chemistry and biochemistry.
- Communication.
- Manufacturing.

2.4 Microwave and Millimeter wave interaction with GDDs

Microwave and millimeter wave detection by GDDs may be explicated by the EM wave-plasma interaction. EM radiations illuminate the glow discharge and heat the free electrons therein thus increasing their kinetic energy. The electrons undergo inelastic collision thereby generating new electrons which also ionize the atoms. The continuous generation of atoms leads to increased discharge current and this is called the enhanced cascade ionization that mostly occurs at the cathode dark space end. Most atoms may be in an excited state during the normal and abnormal modes thus enhanced cascade ionization is easier because of the little energy required. Furthermore, EM waves contribute to this ionization process. In this case, some charged particles

gain energy from the incident EM wave causing diffusion hence a decreased discharge current. This change in the discharge current is [15];

$$\Delta I_d = (\Delta v_i)\mathrm{n} + v_i(\Delta \mathrm{n}) - (\Delta \mathrm{D})\nabla^2 \mathrm{n} - \mathrm{D}\nabla^2(\Delta \mathrm{n}) \quad \textbf{(2.7)}$$

Where v_i is the frequency of ionization collision, D is the diffusion coefficient and n is the density of the electron.

When there is an electric field E, the charged particle motion in the discharge is [16-17];

$$\mathrm{m}\frac{dv}{dt} + \mathrm{vm}v = \mathrm{q}E \quad \textbf{(2.8)}$$

Where m is the mass of the charged particle, v is its velocity, v is the collision frequency and q is the electric charge. The "vm$v$ " term gives the of the elastic collisions effect.

For enhanced cascade ionization, (2.8) maybe modified to;

$$\mathrm{m}\frac{d(\Delta v)}{dt} + \mathrm{vm}\Delta v = \mathrm{q}E \quad \textbf{(2.9)}$$

Where Δv is the change in the velocity of the electron resulting from EM radiation. The EM wave electric field should be in the same direction as the change in velocity.

The gain in the kinetic energy by the electromagnetic wave is the same as the work done by the electric field on the charged particle and by Poynting's Theorem, the rate of gain in the kinetic energy can be written as;

$$\int_V (\mathrm{E}\cdot\mathrm{J})\mathrm{dV} = -\oint_S (\mathrm{E}\times\mathrm{H})\mathrm{dS} - \frac{\mathrm{d}}{2dt}\int_V (\epsilon E^2 + \mu \mathrm{H}^2)\mathrm{dV} \quad \textbf{(2.10)}$$

The right-hand-side first term is the rate of the energy flow through the boundary surfaces and the second term is the change in the electric and the magnetic field energy. The left-hand-side term is the energy change for particles in volume V per unit time [18-19].

It should be noted that the transmission of EM radiation in plasma is dependent on plasma frequency (directly proportional) [20-21].

It is also noteworthy that the rate of change of kinetic energy is directly proportional to the plasma frequency, the radiation average power and the electron density. In the glow discharge, the electron energy from the incident radiation take part in elastic collisions ionization, as well as excitation and electrons can scatter if this energy is insufficient. The change in the electron energy due to the EM radiation during elastic and inelastic collisions with respect to time is [22];

$$\Delta\in (\mathrm{t}) = \frac{\tau \eta_0 q^2 v P_D}{m(w^2+v^2)}\left(1 - e^{\frac{-t}{\tau}}\right) \quad \textbf{(2.11)}$$

The rate of change of the discharge current is [22];

$$\Delta I_d = \mathrm{q} V_n \mathrm{G} \Delta v_i(\mathrm{t}) \quad \textbf{(2.12)}$$

Where G is the internal gain of the signal and Δv_i is the change in ionization due to EM radiation with respect to time.

The change in the glow discharge current is maximum when the frequency of electron-neutral collision is the same as the incident radiation frequency [22-23] and it has a linear relationship with the incident radiation power.

2.5 A literature review on using neon indicator lamps for detecting microwave and millimeter wave signals

In [24], an experimental survey of the detection properties of different glow discharge detectors for X-band radiation was reported, and comparisons were made with sensitivities of diode detectors with all tubes tested under identical conditions. The tubes were placed in the far field of a 10-dB transmitting antenna with the plane of the electrodes parallel to the RF electric field and perpendicular to the RF energy flow. Even so, there was no receiving antenna used. The detected signal was amplified by 40-dB in a range of 10-100 kHz. A lk resistor was used for biasing. The carrier sine wave was at 9.32 GHz and modulated by 50 kHz. The transmitter power was about 20 mW. Square wave modulation was applied to measure rise time from an oscilloscope and the effective detecting area of the tubes was the product of electrode lengths and separations. The measured and calculated NEPs were ideally identical. It was experimentally deduced that glow discharge lamps have comparable sensitivities to those of diode detectors, when applied as detectors for X-band radiation.

A high sensitivity with inexpensive neon glow lamps was observed at X band frequency in [25]. The signals detected were of 10nW order and the local oscillator power was lower than 10^{-17} W Hz^{-1}. In the experiment, two klystrons were used to generate a signal power of 1.6 mW and a local-oscillator signal power of 1.5 mW and a phase lock loop (PLL) was applied to ensure a constant IF of 50 kHz. The klystrons were tuned to 9.64 GHz. It was essential to stabilize the power supply of the VCO klystron reflector because of the high voltage to frequency sensitivity. This was done by eliminating the low-pass filter because a stable power supply has an integral low-pass filter, and an additional filter may induce some system instabilities. More so, an optical isolator was used to isolate the high reflector voltage from the phase comparator output. The signal was amplified over a bandwidth of 10-100 kHz after. The glow discharge lamps were put in the far field of the transmitting antennas with their electrode plane perpendicular to the microwave electric field and parallel to the microwave energy flow. The NEP values and responsivities were then determined. The responsivities were high due to internal signal gain and the NEP values measured were in the order of 10^{-17} WHz^{-1}.

Low cost glow discharge indicator lamps mounted in a waveguide were experimentally examined as mixers at high X-band LO power levels in [26]. It was ascertained that the conversion efficiency of the IF decreased for LO power levels higher than 30-40 mW, even though there was no damage to the lamps at high power levels. The microwave frequency used in the experiment was 8.69 GHz and the IF was 74 kHz. The test system was based on two sources of 1-W and 18-mW nominal power. An L-band power transistor amplifier of 12W was applied as a driver to an efficient varactor L to X band multiplier. The receiver centered at the IF had a bandwidth of 20 kHz. The noise from the lamp over a 65–85 kHz bandwidth was 23μV. Although after the activation of the RF sources, the noise increased to 26μV. For the 20 kHz bandwidth NEP was 5×10^{-17} WHz^{-1}. The responsivity was about 700 mV. mW^{-1}. When the LO power was increased by 4-dB, there was a corresponding decrease (improvement) in the NEP hence proving the fact of using high LO levels for weak signal detection. However, when the LO level was increased by a factor of ten, the NEP observed was worse.

It was ascertained in [27] that inexpensive neon lamps can not only sense low-power RF radiations but can also accurately determine the incident radiation frequency. In the experiment, a klystron microwave source was modulated by a 2.5 kHz ramp function and the carrier frequency was adjusted by a mechanical tuner. It was reported that the spectral dependence is proportional to $v/(v^2+w^2)$, where v is the frequency of electron elastic collision and w is the incident radiation radian frequency. At a given carrier frequency, the responsivity is at its peak when v is equal to w. It was also mentioned that the electron velocity increases with increase in the potential difference between the electrodes and that the ratio of gas pressure to temperature is independent of the lamp power consumption and remains constant. It was concluded that the use of inexpensive neon indicator lamps for RF sensing is feasible however use of different glow lamps for different spectral regions was recommended.

An experiment was performed and reported in [28], to realize a fast and low-cost millimeter wave glow discharge video detector. It was ascertained that when a glow tube is biased properly, it demonstrates a sensitivity that corresponds to that of a crystal diode detector. In the experiment, electrodes from an NE2 glow lamp were placed in the experimental tube. The tube was evacuated to 10^{-6} torr pressure between gas fillings. Gases tested included neon, helium, xenon and argon. The carrier signal was 70 GHz from a 70-V 11A E-band klystron source and

was square-wave modulated by a 1 kHz wave. The gas in the tube was broken down by a dc between the electrodes. The load resistance was made up of a fixed 10 kΩ current-limiting resistor in series with a 200 kΩ potentiometer applied to alter the discharge current. The following conclusions were made from the experiments;

- Sensitivity in GDDs with pure gases depends on using light gas.
- Noise and Responsivity in GDDs increase with mass, although at different rates.
- To have an increased potential gradient between the electrodes, the separation between them must be reduced.
- GDD biasing greatly affect the detector efficiency and is normally different for different carrier frequencies.
- For 0-150 kHz range, the noise spectrum for most 2-electrode tubes has a maximum at lower frequencies and a minimum at higher frequencies.
- THz signals can be detected using an external electrode taped to the glow discharge tube.

The impact of THz radiation polarization on the GDD responsivity was examined in [1]. The experiment was carried out using GDD neon indicator lamps and enhanced cascade ionization proved to be the prevalent detection mechanism. It was posited that when the THz radiation electric field is in the same direction as the DC bias electric field of the GDD, the responsivity is about 50% higher than when it is orthogonal. In the experiment, a head-on configuration was used since it enabled the authors to rotate the GDD to see different incident THz polarizations and enabled greater interaction of the THz radiation with plasma and hence having good responsivity. The THz source used was an ordinary 2-18 GHz synthesizer and was multiplied to have 92-102 GHz by GaAs multipliers. The radiation power levels were 150–200 mW. The radiation was let to free space by a waveguide and a horn antenna and the THz polarization was according to TE_{01} mode of the waveguide. The GDD was fixed in a rotation holder to be rotated from 0° when the DC electric field is in the same direction as the THz electric field and to 90° when the fields are orthogonal to each other. The radiation was focused onto the GDD by a polyethylene (PE) lens and the signal was captured by an oscilloscope which was controlled by a computer code and a GPIB communication protocol.

The performance of neon lamp GDDs at 0.2 THz was investigated in [2]. The authors constructed a THz CW imaging system and the images obtained were compared to those of a Schottky diode. The experimental results showed that a well-designed GDD is a potential candidate for THz imaging systems detection. The CW THz source used was a Gunn diode which gave a 0.2 THz beam with 40 mW power. The beam was modulated at 900 Hz and then focused on the sample by a high-density polyethylene (HDPE) lens of 66 mm focal length and then on the GDD electrode gap by another HDPE lens of the same focal length. A motorized scanning stage was applied to scan the sample. An oscilloscope and a spectrum analyzer were used to test the GDDs' performance. At a modulation frequency of 900 Hz, the NEP and responsivity were 1.26×10^{-8} W/Hz$^{1/2}$ and 55 V/W respectively with a discharge current of 9 mA. The spatial resolutions were 1.65 and 2.05 mm for the GDD and Schottky diode respectively.

The interaction of GDDs with THz radiation using terahertz time domain spectroscopy (THz-TDS) in a range of 0.05 and 0.5 THz was examined in [29]. Results showed that the GDD structure plays a significant role in the detection mechanism. It was observed that transmission at a specific frequency can be reduced and as well tuned with increased bias voltage on the gap thus the devices could be applied as hybrid plasma filters. In the setup, a fiber laser output was split into THz pulse generation and detection parts by a beam splitter. In the generation part, the beam was focused onto a photoconductive dipole antenna (PCA) fed by a generator of 20 V peak-to-peak and square modulated at 1 kHz. The THz pulse was then collimated by an off-axis parabolic mirror (OAP) of 50 mm diameter and focused onto the sample by two confocal plano-convex Teflon lenses of 50 mm diameter each, and then by another OAP onto the electro-optic detection crystal. In the detection part, the linearly polarized beam was delayed by a delay stage and then let to the detection crystal. Thereafter, the elliptically polarized beam was passed through a quarter-wave plate and a Wollaston prism. Results showed that the GDDs behave like a band-stop filter with decreased transmission for increased applied bias before breakdown. Thus, by altering the gap and lead thickness the resonant frequency can be adjusted to low and high frequencies in the low-frequency THz region which justifies the potential role of these devices in THz application as tunable hybrid-plasma filters.

Focal plan array (FPA) imagers based on low cost neon indicator lamp GDDs were developed and reported in [30]. The technic developed cancelled out differences in FPA lamps response brought about by non-uniformity of the GDDs and mmW collimated beam as well as other electronic components. Utilizing this method in the new imaging system unifies the detector response. Results showed better performances with two sensor configurations (8×8 and 18×2 scanner array). A 100 GHz source of GaAs multipliers was used to step up a low frequency source of 12.5 GHz. Both configurations' sources were amplitude modulated by a 100 kHz sinusoidal and the signal was let to free space by a horn antenna. The quasi optic systems were the same for both configurations and were set up to image as per optics principles. For system optimization, ZEMAX software was used. It was concluded that by calibration and oversampling, inexpensive GDD FPAs can allow real time good image quality when all detectors are illuminated simultaneously.

The impact of the aging of the neon indicator lamp GDD on its responsivity was experimentally examined in [31], and a circuit for fast electronic ON/OFF switching was demonstrated. In this experiment, a 93 GHz signal with 400 mW power was generated and it was focused between the electrodes of the GDD by a lens, a parabolic mirror and a pyroelectric array camera. The beam diameter was 9 mm with a power of 90 mW. The incident radiation power on the GDD was 3.9 mW with a noise voltage of 200 nV/√Hz. The GDD response was 80 mV at 10 kHz modulation frequency which resulted in a responsivity of 20.5 V/W. The NEP was 10 nW/√Hz. It was concluded that switching on the GDD bias current for the detection period only, not only increases the detector lifetime, but also increases the lifetime of its responsivity thereby curbing the aging effects. For n GDD pixels, the time for the GDD to be switched on is n-1 of each frame period, hence reducing the effects of heating and aging. More so, improvements may also be realized by switching the operating voltage polarity for successive GDD on/off detection.

An inexpensive technic to obtain a 3D millimeter wave image using up-conversion was presented in [32]. The authors described and demonstrated an up-conversion method of THz radiation to the visual band using a low-cost miniature GDD (N523) and a silicon photodetector by measuring the visual light from the GDD instead of the electrical current and results showed improved response time and sensitivity. More so, FMCW radar detection was performed using a GDD lamp and a photodetector. The GDD acted as a mixer electronically and optically. In the

experiment, a THz source based on multipliers was used to generate a 100 GHz signal and was modulated by a 1 kHz square wave. It was concluded that in electronic detection, response time limitations are as a result of GDD parasitic capacitance and inductance. Because of up-conversion, the GDD output is an optical wave instead of a current, therefore the parasitic impedance is removed from the output, and the detection speed largely depends on the optical detector speed. Likewise, the sensitivity of electronic detection is limited by the GDD noise and with up-conversion, this is also removed and thus sensitivity becomes dependent on the noise of the optical detector, which is less than the GDD noise. Hence, detection speed and sensitivity can be significantly improved using a faster and quieter detector or optical camera.

A 300 GHz heterodyne detection technic using GDDs was experimentally examined in [33] and a comparison to direct detection was also made. Results showed improved sensitivity with 56 μW LO power. In the experiment, two synchronized THz sources at 300 GHz and 300 GHz+Δf based on multipliers were used and were let to free space by conical and diagonal antennas respectively. An OPM was used to focus the beams between the GDD electrodes and the GDD was connected to a detection circuit with a low-noise preamplifier of 100 voltage gain and a band-pass of 20 kHz and then to an oscilloscope. Side-on configuration was used and the measured GDD glass envelope transmission function at 300 GHz was 60%. It was concluded that the ability of GDDs at 300 GHz enabled more sensitive THz imaging and results suggested that FPAs need to be put into consideration for heterodyne THz imaging systems since imaging at 300 GHz provides better resolution although high LO power is required.

In [34], GDDs' performance at 10 GHz in direct detection and heterodyne detection was compared. Experimental results showed that heterodyne detection is more sensitive by nearly two orders of magnitude than direct detection, and that sensitivity is inversely proportional to increasing LO power. In the experiment, two 10 GHz synthesizers were used with one modulated for direct detection and the other being a constant CW generator. Both beams were CW for heterodyne detection, and the IF signal was detected whereas only one source was used for direct detection and the beam was amplitude modulated. It was concluded that heterodyne sensitivity with GDDs is inversely proportional to the LO power, and signals were successfully detected using heterodyne detection at lower levels than with direct detection.

Glow discharge plasma, from dc gas breakdown, was investigated in [35] to realize a low-cost THz detector. Results showed that for THz radiation, GDDs (N523 neon indicator lamps) have good responsivity and NEP. It was argued that it is advantageous to develop FPAs using these GDDs since FPA images are limited by diffraction. The detection mechanism of the GDD was the enhanced diffusion current, which caused the GDD bias current to decrease when subjected to THz radiations. 100 GHz and 250 GHz sources were used based on GaAs multipliers with a 0-18 GHz synthesizer as the low-frequency source, modulated by a 1kHz square wave with 150–200 mW radiation power. The GDD operated in the abnormal glow region of the current voltage characteristics. The GDD dc current was 3 mA.

CHAPTER 3

METHODOLOGY

3.1 Research Methodology

The primary objective of the research was to detect both microwave and millimeter wave signals using an AC driven GDD because of its advantages which include but not limited to; low cost, faster response time, electronic ruggedness, wide dynamic range, broad spectral range and potential to operate at high temperatures.

Nevertheless, as literature survey was done, specific objectives were realized which included; biasing the GDD with alternating current (AC), examining the relationship between the modulation frequency and the peak to peak voltage of the received THz signal, analyzing the signal before and after filtering and amplification, analyzing the GDD responsivity with respect to time as well as examining the effect of the distance between the microwave signal source and the GDD. Thus, an experimental research methodology was used for this thesis.

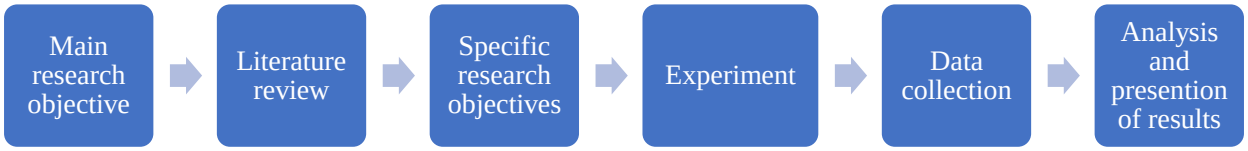


Figure 3.9 Research Methodology

Our research was approached using the above steps, whereby after identifying the main objective, a thorough literature review was conducted to get a comprehensive insight of the subject and realize the specific objectives. This included reviewing journal papers, conference papers, text books, theses as well as using various websites' articles. Thereafter experiments were performed in the lab, and data was collected, analyzed and presented.

3.2 Experimental setup

Two experiments were performed; millimeter wave/THz and microwave detection and in this section, we comprehensively describe the steps that were taken to set up the experiments.

3.2.1 Millimeter wave/THz detection

To detect THz signals using an AC driven GDD, the following was needed:

- A GDD
- An AC source to bias the GDD
- A THz signal source and modulation
- Filters
- An amplifier
- A scope for monitoring the detected signal

3.2.1.1 The GDD

The GDDs used in our case were neon indicator lamps of NE-2 series because of their advantages mentioned earlier. It should be noted that the characteristics of an ac glow discharge ideally depends on the gas type and its pressure as well as the electrodes' geometry and their material. Even so, the electrodes are normally coated with barium azide or barium strontium oxide (because of their higher electron emission coefficients) to lower the required breakdown voltage.

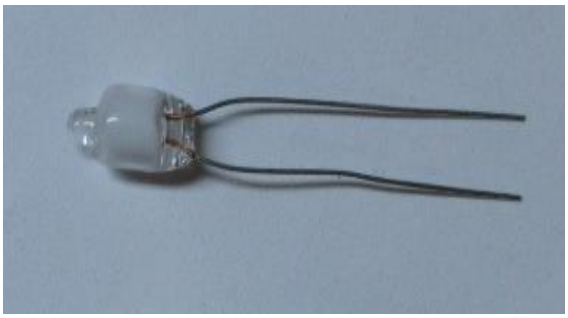


Figure 3.10 The GDD used

3.2.1.2 The Biasing circuit

The GDD was biased using an AC source as shown in the figure below. With AC biasing, charge during one half cycle is neutralized by the opposite charge in the next half-cycle. In this case the role played by the cathode and anode changes alternately. It should be noted that an alternating voltage applied between electrodes can help to alleviate the problem with dc glow discharge where electrodes may charge up when one of the them is non-conducting due to the constant current, thereby causing the glow discharge to burn out. In our experiment, the GDD was biased using an 11kΩ resistor connected in series with the GDD and an AC from a transformer of 110V output voltage which is about 155Vp (peak voltage). However, the measured peak value was 158V giving a peak to peak of 316V. The transformer was a T11500B-FE model from Artsanenerji.

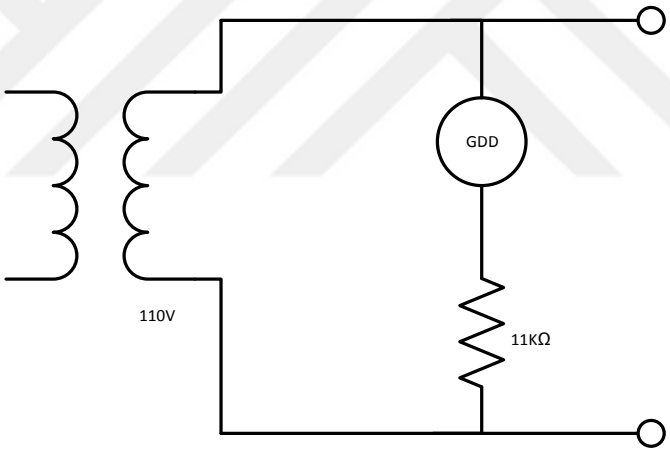


Figure 3.11 The Biasing circuit

3.2.1.3 Millimeter wave/THz source

The millimeter wave signal was generated by a VDI frequency multiplier, which multiply the low frequency RF synthesizer frequency to 60 GHz. The signal was emitted to the GDD by a horn antenna. The signal was then modulated with different frequencies and for our case 170kHz proved to be the most efficient.

3.2.1.4 The filter

To get rid of the 50 Hz AC frequency and other noise, passive LC high-pass filters were added. It should be noted that LC high-pass filters are used in a spate of applications where they tend to bar low frequencies and admit through high frequencies. Passive LC filters are ideally used for high frequency signals where active filters may not be manageable. The figure below shows the filter circuit used. The capacitors used were 22.3nF and 0.56nF for the first and second filters respectively and inductors were 3.3mH for both filters giving a cutoff frequency of 18.55kHz and 117.08kHz respectively.

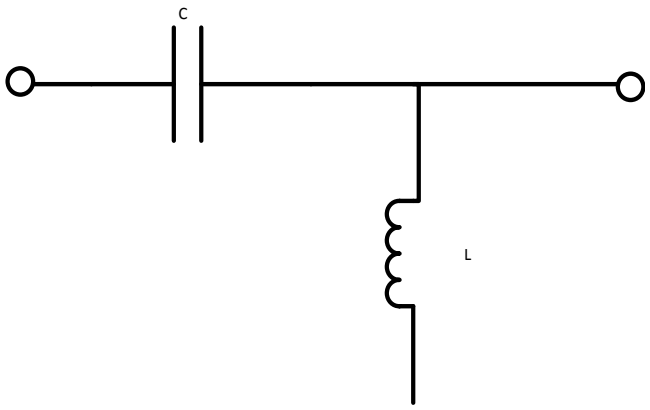


Figure 3.12 The filter circuit

3.2.1.5 The amplifier

After the signal passing through the filter, it was amplified so that it could be visible on the oscilloscope. The schematic diagram of the amplifier used is given below. The diodes were used to shield the operational amplifier (op amp) from plasma voltage fluctuations. Even so, the op amp was driven by a 9V source since this is usually one of the standard voltages from batteries. Batteries are normally used to drive the op amps since they give less noise. The regulated power supply used was an ATP-3303D model. The op amp used was an LM324N because of its advantages which include; low noise, high speed and low offset voltage. The input, bandwidth and the impedance of this op amp do not affect temperature coefficients and manufacturing variations.

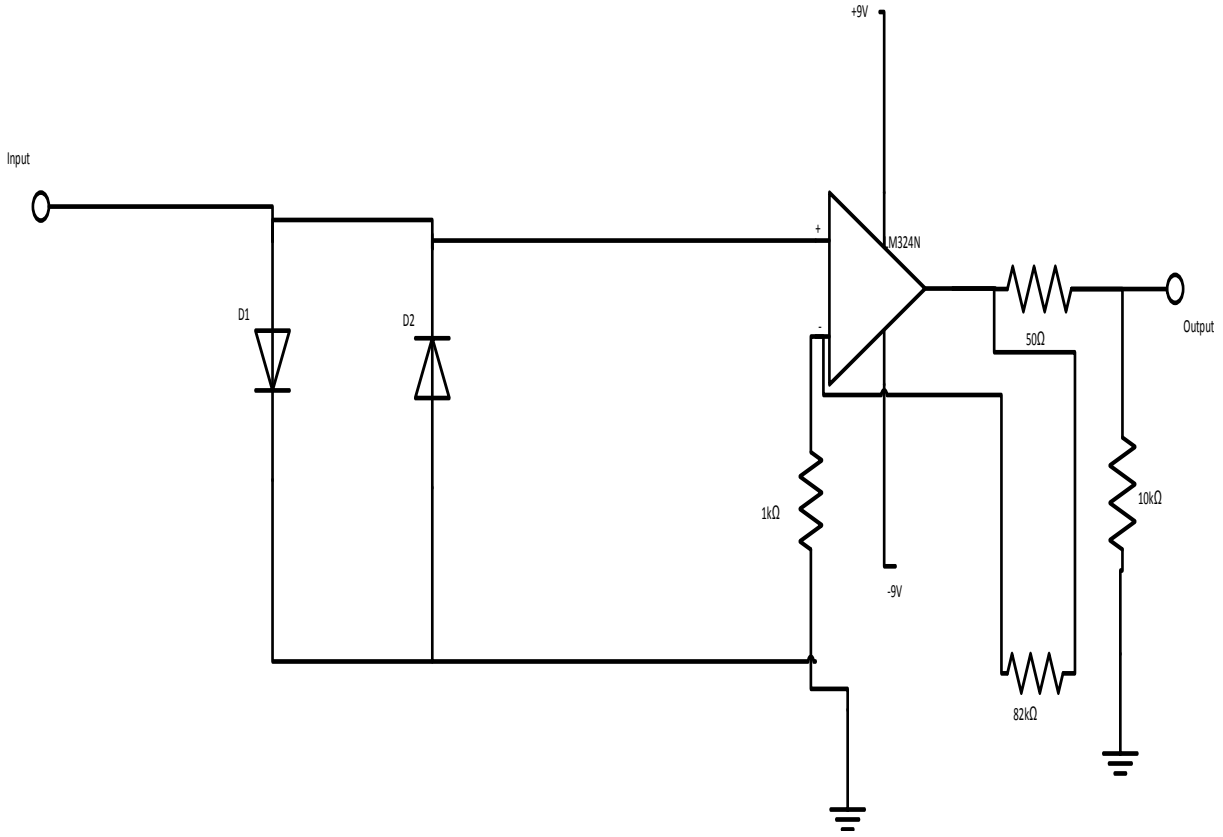


Figure 3.13 The amplifier circuit

To effectively detect the THz, signal a secondary filter was used after the amplifier, thenceforth the THz detection experimental setup was as below;

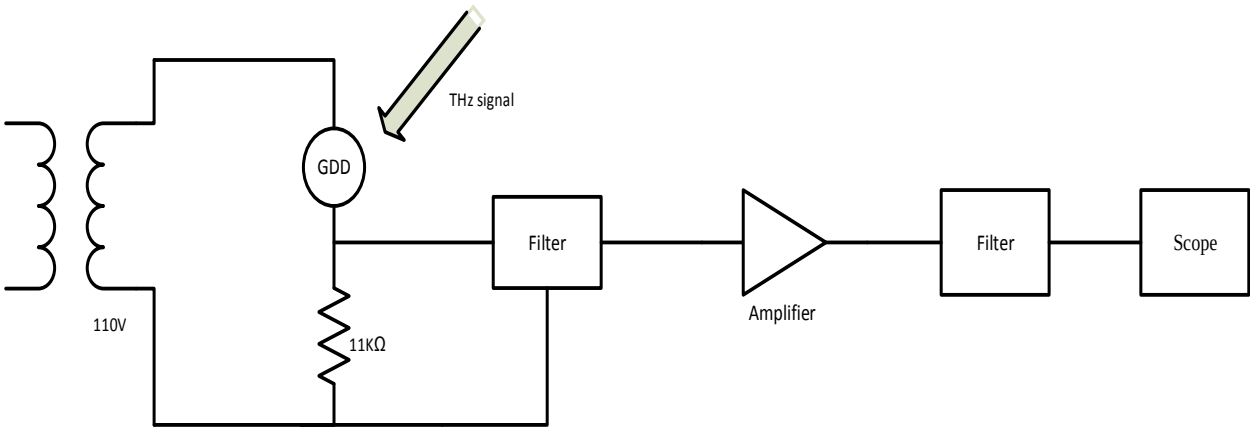


Figure 3.14 The schematic diagram for the whole setup

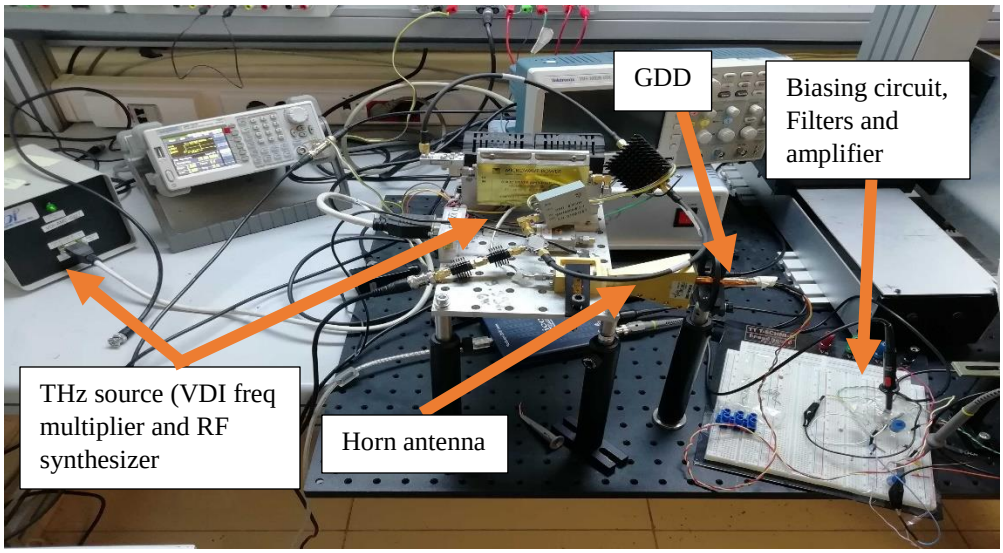


Figure 3.15 The experimental setup

3.2.2 Microwave detection.

To detect microwave signals using an AC driven GDD, the components used in THz detection were used.

3.2.2.1 The microwave signal source and modulation

A microwave doppler sensor of X-band frequency (10.5GHz) was used to emit a microwave signal to the GDD. Notably, side configuration was used in the experiment instead of a head-on configuration. Microwave doppler sensors have the following features;

- High sensitivity
- Low power consumption
- Small in size
- Rugged reliable construction
- Pulse mode and CW capabilities
- Temperature ranges of -10°C to 55°C
- Patch antenna

The signal was modulated using different frequencies and measurements were taken. 200kHz and 250kHz proved to be the most efficient modulation frequencies.



Figure 3.16 The microwave doppler sensor used

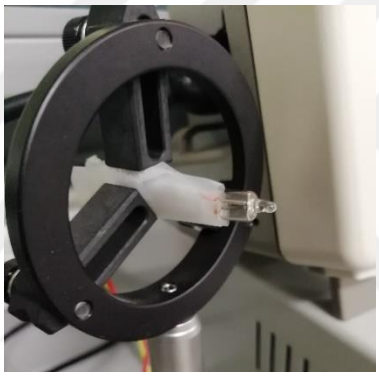


Figure 3.17 GDD used for microwave detection

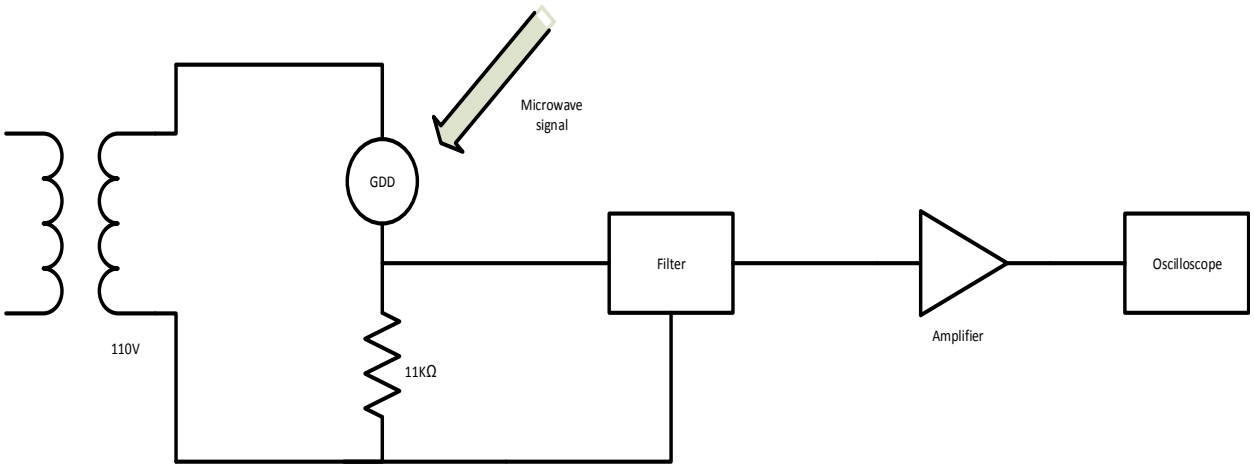


Figure 3.18 The microwave detection schematic

CHAPTER 4

RESULTS

4.1 THz Detection

In our experiment, the THz results were captured using a Pico scope and nevertheless, Microsoft excel, and MATLAB were used for analysis.

4.1.1 Signal modulation

In the experiment, the THz signal was modulated using different modulation frequencies and 170kHz was found to be the most efficient modulation frequency and hence it was used to modulate the THz signal throughout the experiment.

4.1.2 Signal detection before filtering

At this stage, the voltage across the load (Rload) and the AC signal voltage were captured with and without the THz radiation as shown below;

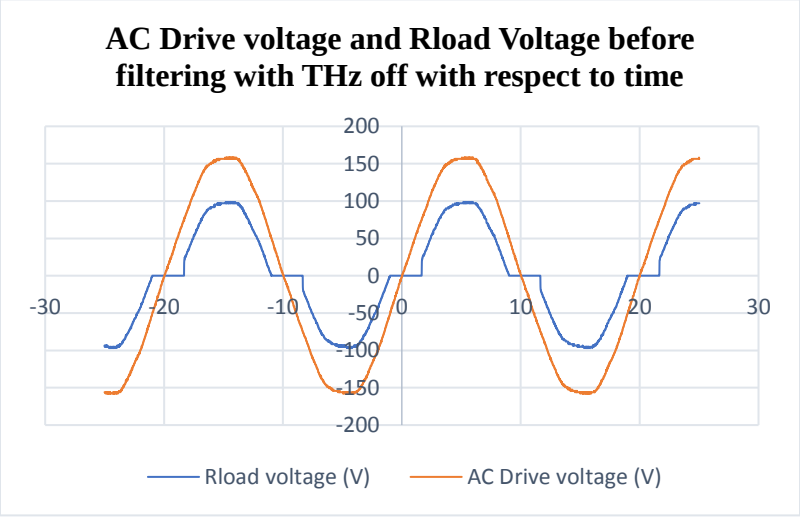


Figure 4.19 AC drive voltage and Rload voltage with THz off

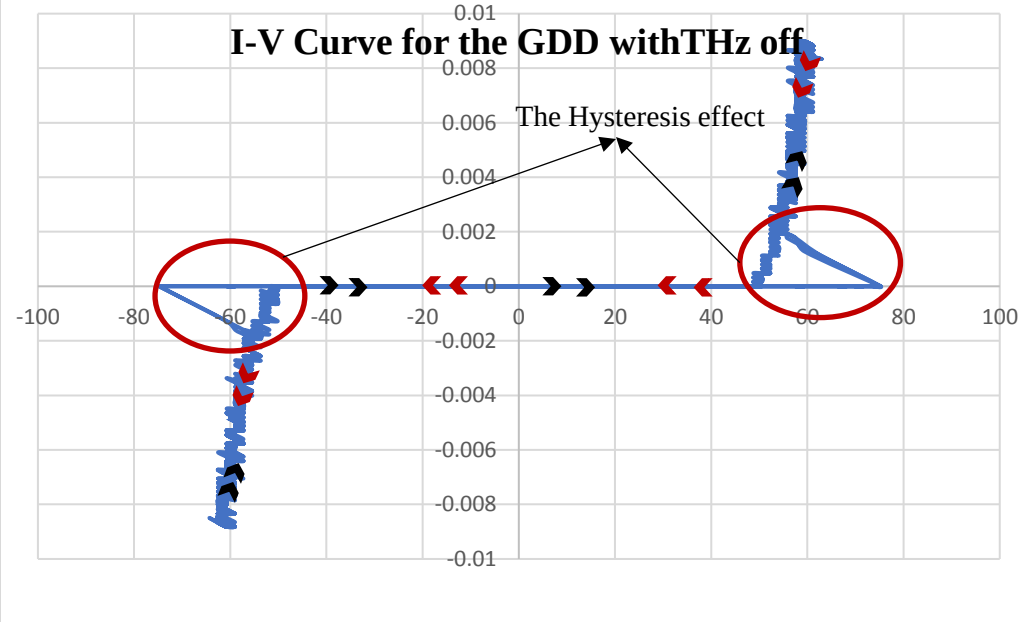


Figure 4.20 I-V Curve for the GDD withTHz off

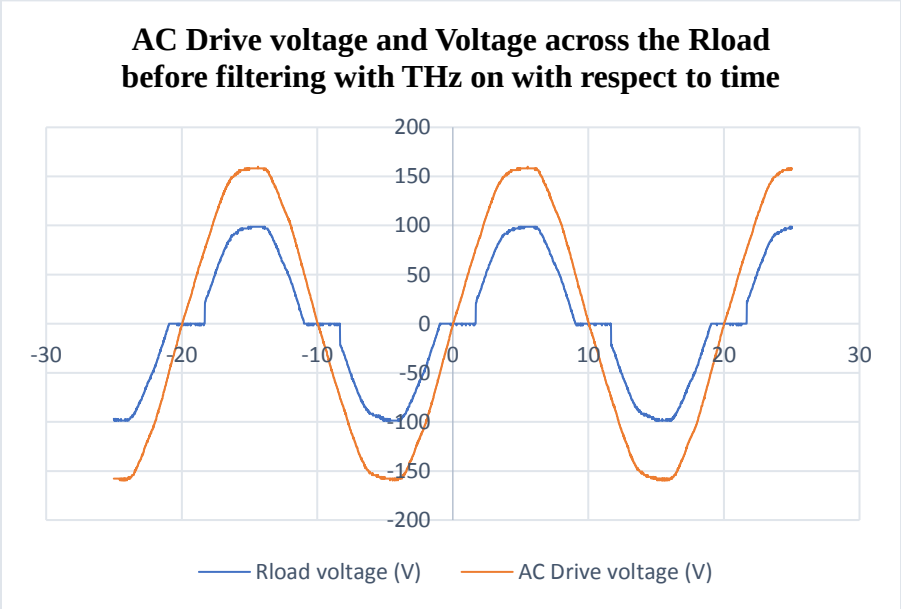


Figure 4.21 AC drive voltage and Rload voltage with THz on

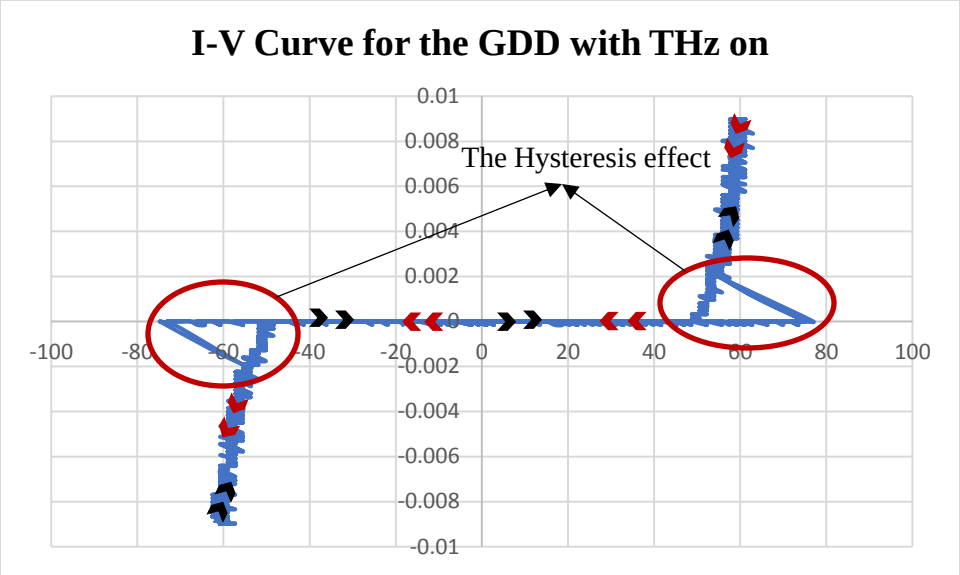


Figure 4.22 I-V Curve for the GDD with THz on

As it can be depicted from figures *4.19* and *4.21*, the AC peak to peak voltage is 316V and the peak to peak voltage on the GDD is 200V. The GDD is turned on at around 60V AC and is off when the AC drive voltage is at around 30V in the positive half cycle and also in the negative half cycle.

Furthermore, figures *4.20* and *4.22* show the I-V characteristics of the used GDD. It can be depicted that current increases exponentially after turn-on with respect to voltage. Nevertheless, the circled regions show the hysteresis effect which is the difference between the pinch-off and turn-on voltages whereas the black and red arrows show the increasing and decreasing rate respectively

Driving the GDD with alternating voltage helps to curb the problem with DC driven GDDs whereby the accumulated charge in the first half cycle, is neutralized by its opposite in the succeeding half-cycle. In this case the role of the anode and the cathode is changing alternately. Hence, there is no instance when either the cathode or the anode is non-conducting as it is the case with DC biased GDDs because of the fact that the current is constant which leads to GDD burn-out.

The figure below shows the relationship between the received signal magnitude and the GDD current (I_{GDD}) from which the responsivity of the GDD can be derived.

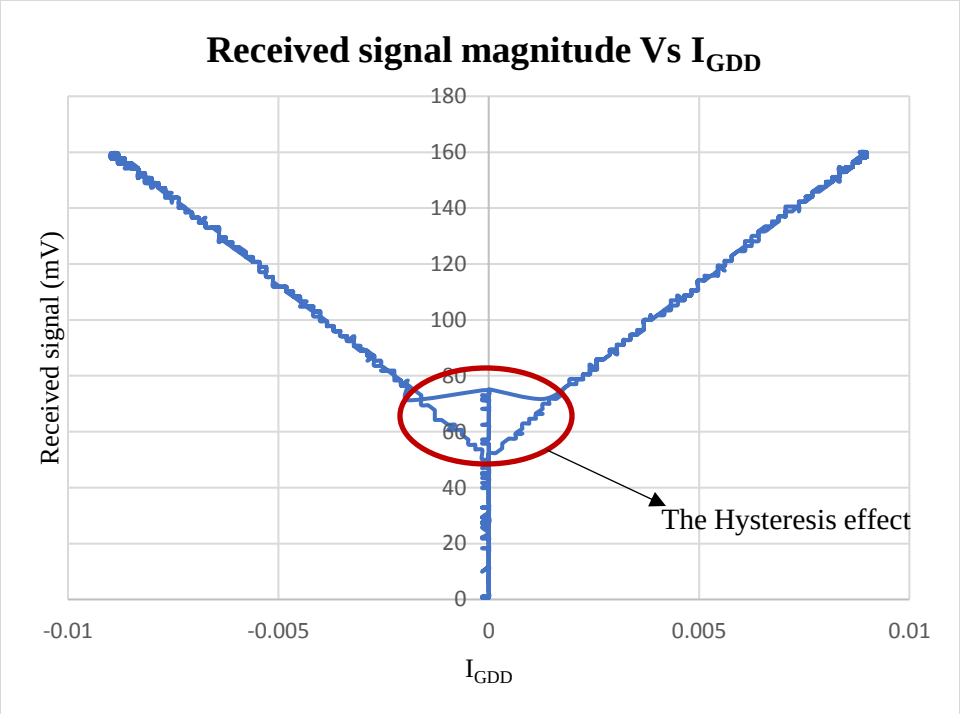


Figure 4.23 Received signal magnitude versus I_{GDD}

$$Responsivity\ (R) = \frac{measured\ voltage}{power\ input} \quad \textbf{(3.1)}$$

In our case the power input is 300mW (60GHz), the slope of the curve is 0.0142 and I_{GDD} is 1.8mA.

Hence, $R = \frac{52}{300} + (0.0412 \times 1.8) = 0.25\,\frac{mV}{mW}$ **(3.2)**

4.1.3 Signal detection after first filtering

In our experiment we applied a high pass filter to get rid of the noise as explained in the preceding chapter. The signal received as well as the ac driving voltage with the THz source off as well as when it's on are depicted in the figures below;

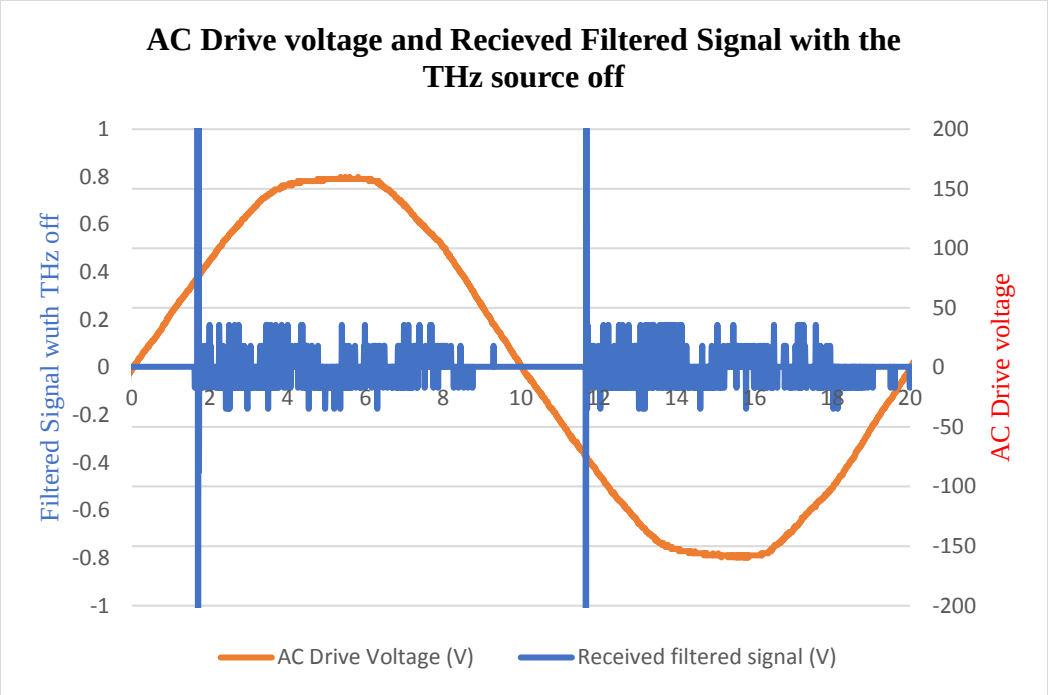


Figure 4.24 AC Drive voltage and Received Filtered Signal with the THz source off

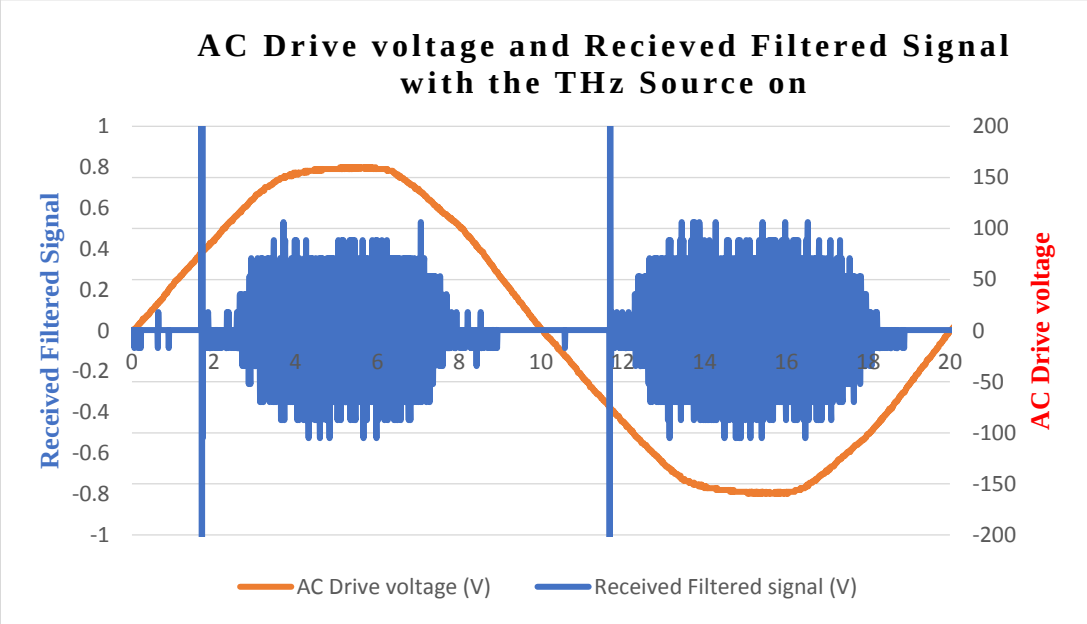


Figure 4.25 AC Drive voltage and Received Filtered Signal with the THz source on

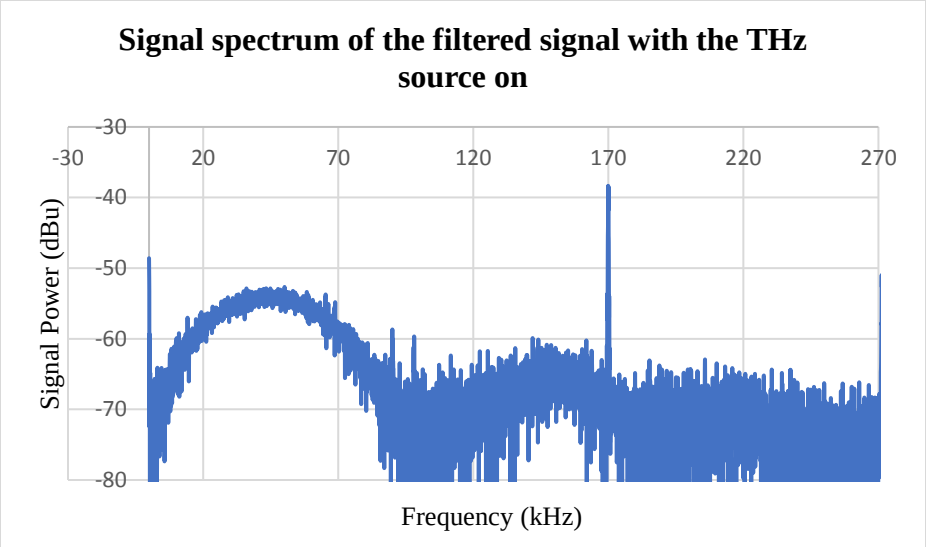


Figure 4.26 Signal spectrum of the filtered signal with the THz source on

As it is clearly depicted in the figures above and the corresponding signal spectrum, the filtered signal was too weak (-38dBu) and there was still some significant noise especially at lower frequencies that it needed amplification and further filtering. Hence an amplifier with specifications explained earlier was used and the ensuing amplified signal is expatiated in the following section.

4.1.4 Signal detection after amplification

During the experiment, the signal was amplified using an amplifier with specifications posited in the preceding chapter and results were taken with both the THz source and the AC drive voltage on, as shown below.

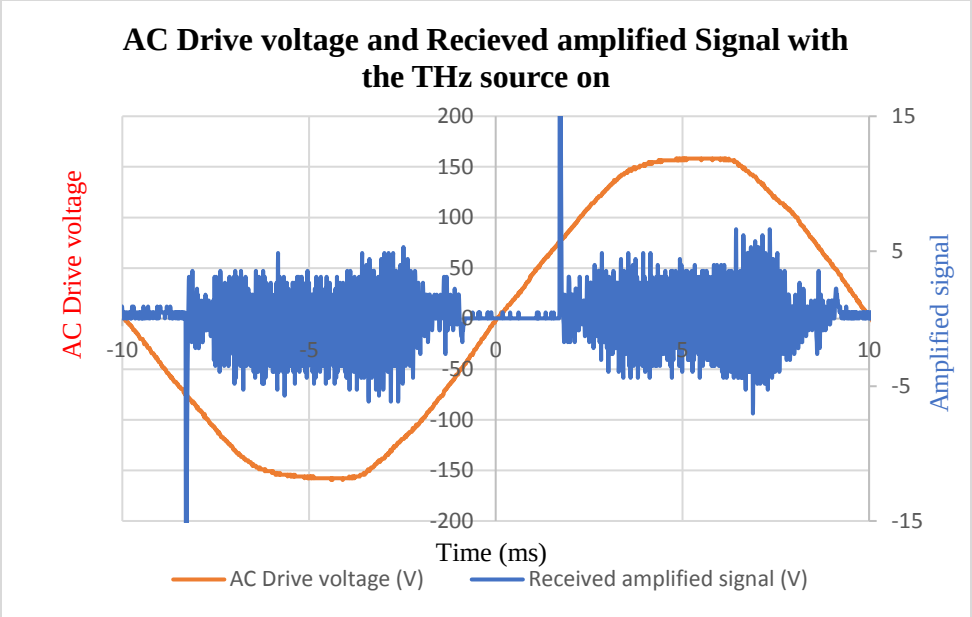


Figure 4.27 AC Drive voltage and Received amplified Signal with the THz source on

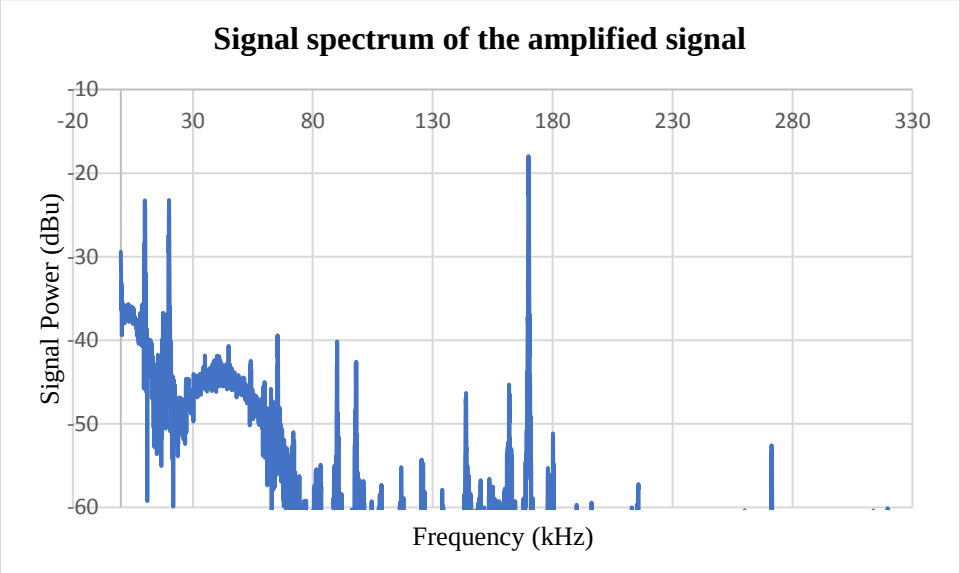


Figure 4.28 Signal spectrum of the amplified signal

As it is illustrated from the figure above, the signal was amplified by approximately 20dB at 170kHz which our frequency of interest was.

However, it should be noted that the amplifier was amplifying both the required signal and the noise. Thus, there was need for a secondary filter to get rid of the noise.

4.1.5 Signal detection after secondary filtering

A narrower secondary filter was used to get rid the of noise which was majorly from the dc power supply to the op amp which was around 24mV as shown in figure, and this helped to get a cleaner signal.

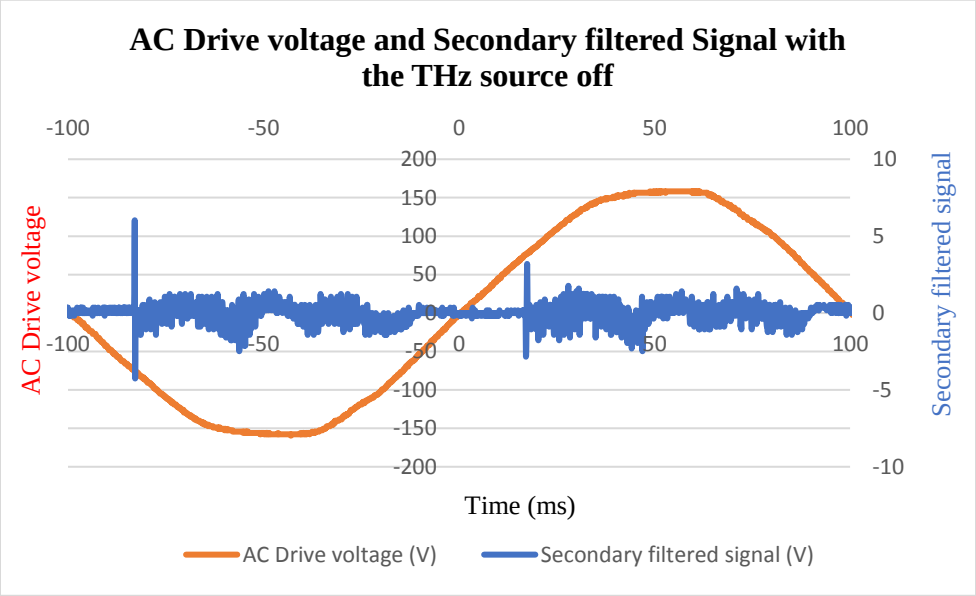


Figure 4.29 AC Drive voltage and Secondary filtered Signal with the THz source off

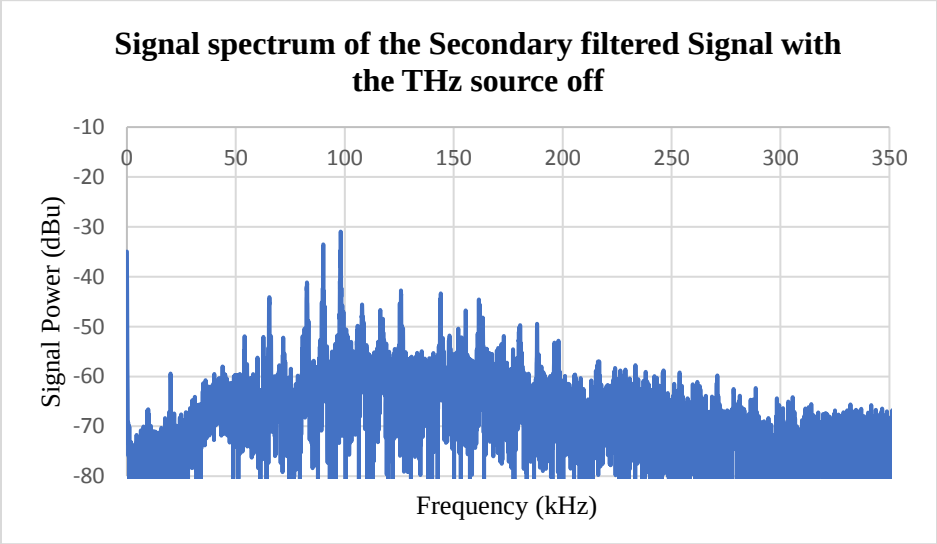


Figure 4.30 Signal spectrum of the Secondary filtered Signal with the THz source off

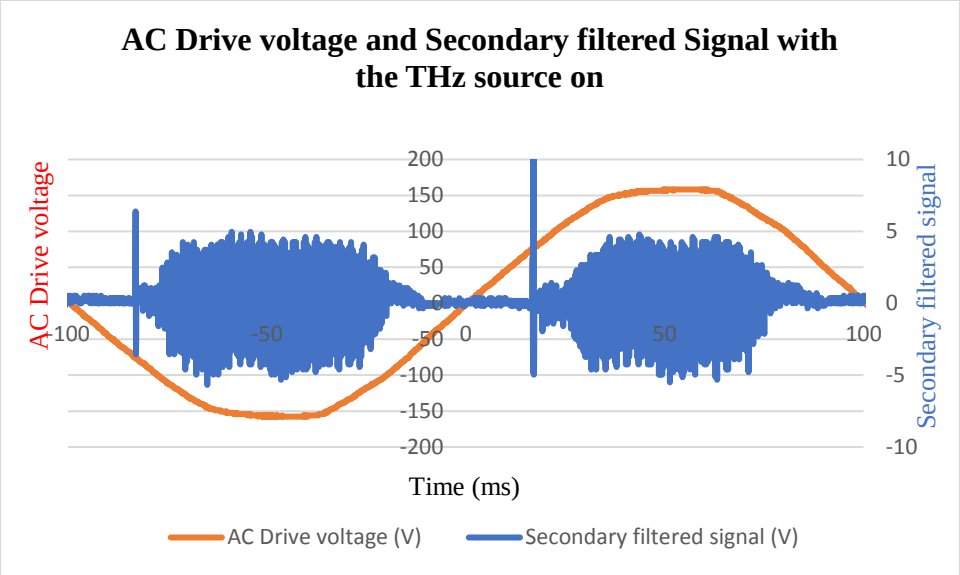


Figure 4.31 AC Drive voltage and Secondary filtered Signal with the THz source on

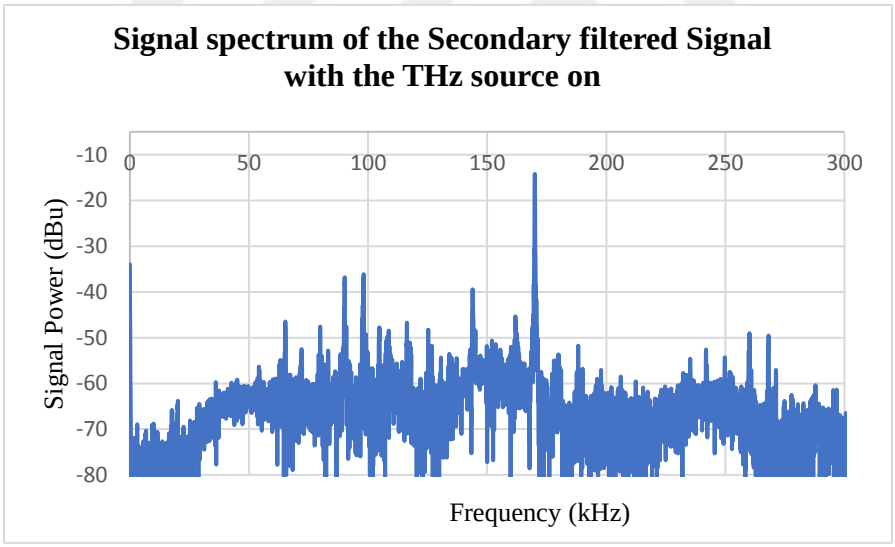


Figure 4.32 Signal spectrum of the Secondary filtered Signal with the THz source on

Below is the dc noise spectrum and its FFT was majorly from the dc power supply to the op amp which was around 24mV.

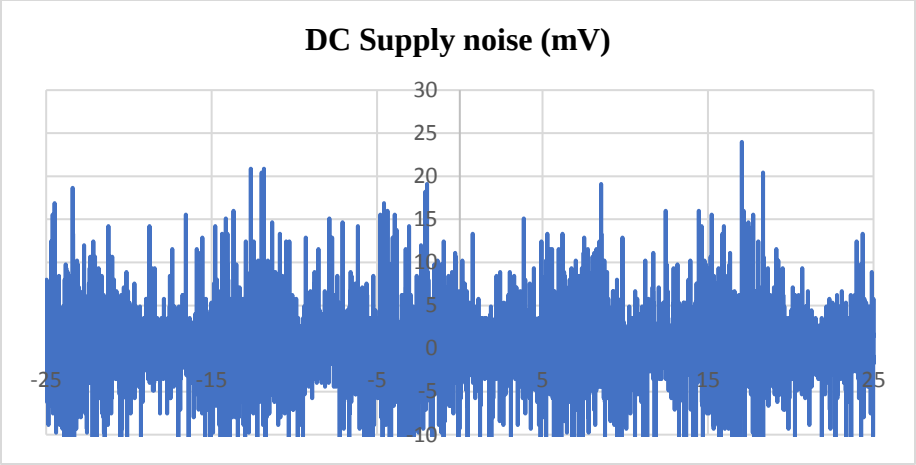


Figure 4.33 DC Supply noise

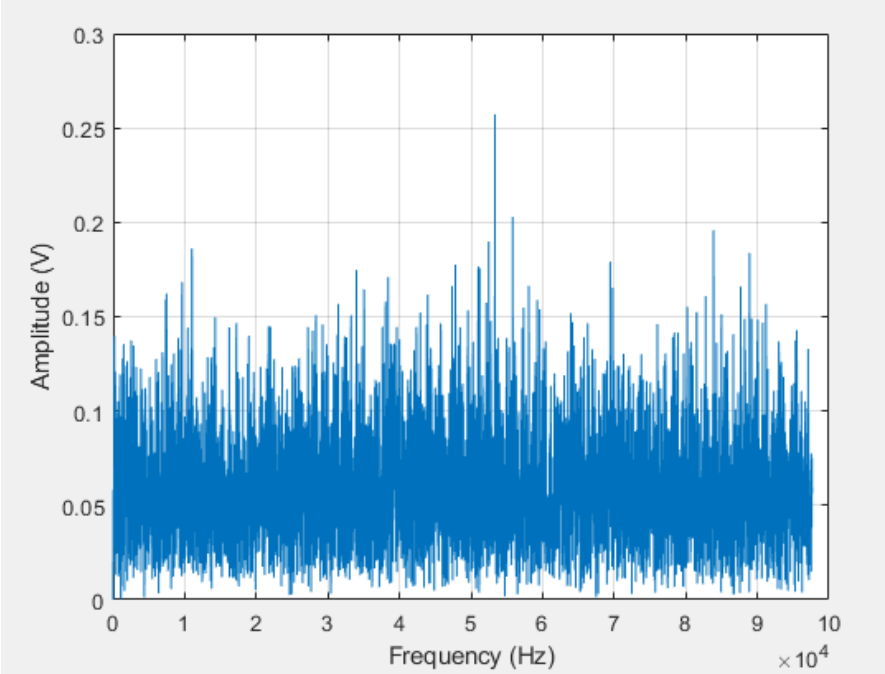


Figure 4.34 FFT for DC supply noise

As it can be seen from the figures above, the filter used helped to get rid of the noise at lower frequencies. Hence using narrower filters can significantly help with signal cleansing.

4.2 Responsivity of a DC driven GDD

The continuous operation of a GDD in the abnormal glow realm ruins its electrodes (particularly the cathode) with time, and this is so because of the step-up in positive ion bombardment. This therefore leads to the diminishing of a GDD's responsivity. We proved this experimentally whereby we measured the responsivity of a DC driven GDD for 10 minutes. A DC voltage of 158V was applied to the GDD with 9mA of current passing through it. The response was as shown below.

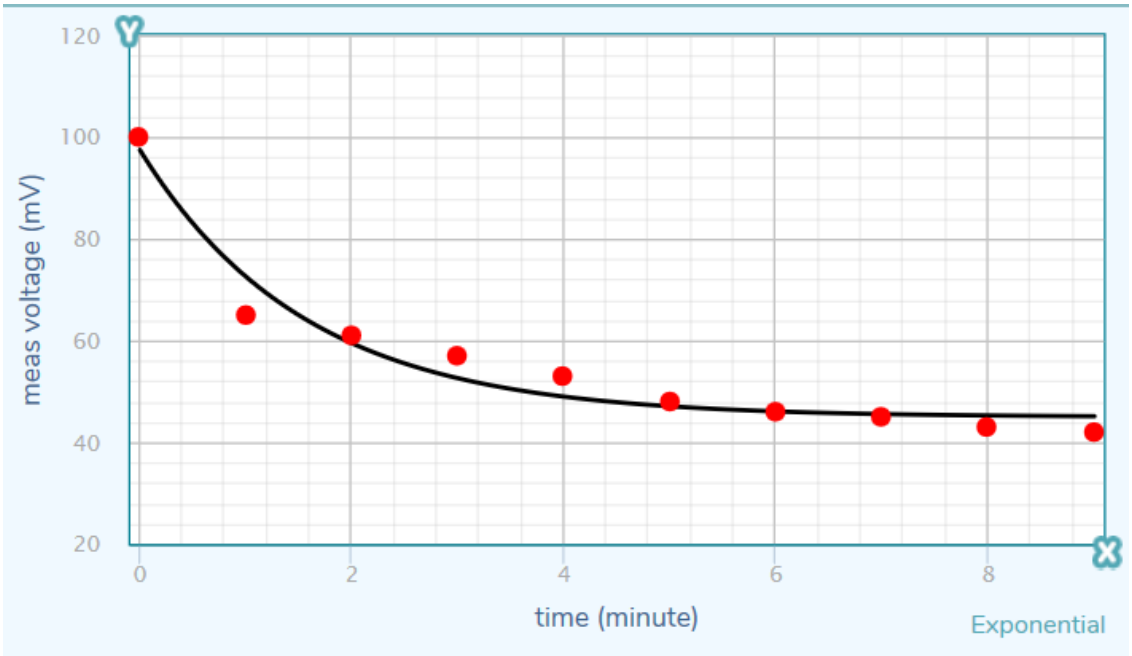


Figure 4.35 Responsivity decay for a DC driven GDD

It was observed that at the switch-on instance, the responsivity was 100mV and after 9 minutes it was 42mV. The responsivity decay was 96% consistent with the exponential curve equation; $y = a + be^{-cx}$ where a=44.95 steady state value, b=52.46 transient value, c=0.64 the decay rate in minute^{-1}, and x was the time in minutes. Hence for this particular GDD, responsivity decreased to 45% of the maximum value in as fast as 9 minutes.

4.3 Effect of the modulation frequency on the detected microwave signal

A second experiment was performed during which a microwave signal was modulated with different modulation frequencies and the respective peak to peak voltages were recorded as shown in the table below. It was observed that 200kHz had the highest peak to peak voltage of 2.8mV followed by 250kHz with 2.6mV. A steady decrease in the peak to peak voltage of the detected signal between 30kHz and 100kHz was observed while a steady increase was observed from 100kHz to 200kHz. Thereafter, a decrease was again observed. The distance between the GDD and the signal source was 5.4cm and it was arbitrary. Thus, it can be deduced that to detect a microwave (X-band) signal using a GDD, its more efficient to modulate the signal with 200kHz.

Table 4.3 Modulation Frequencies versus voltage for Microwave

Modulation Freq (kHz)	Vpp (mV)
10	2
20	1.8
30	2
40	1.8
50	1.4
100	1.6
150	2.4
200	**2.8**
250	2.6
300	1.8

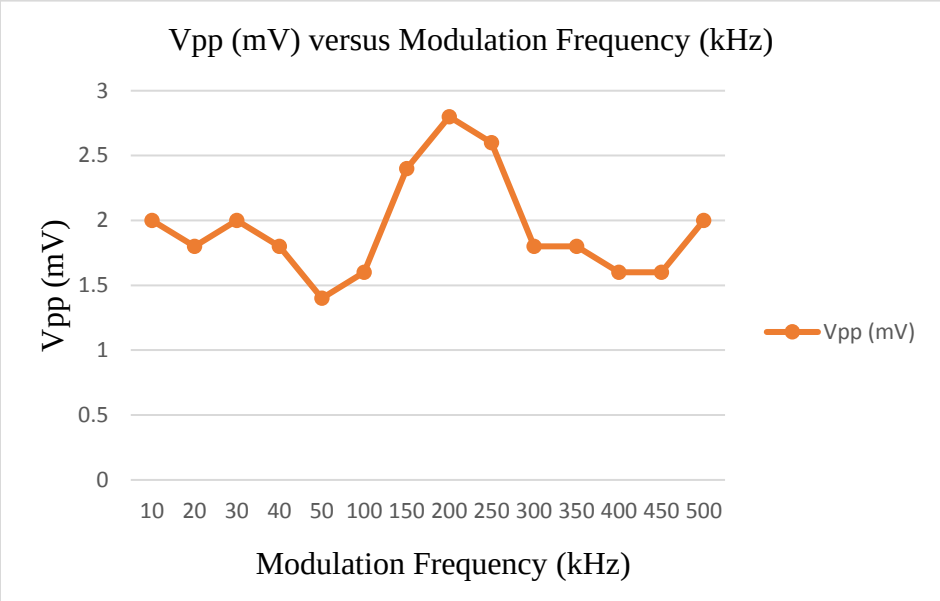


Figure 4.36 Vpp (mV) versus Modulation Frequency (kHz) for microwave

4.4 Effect of the distance between the GDD and the signal source on the detected microwave signal

After ascertaining the most efficient modulation frequencies (200kHz and 250kHz), the distance between the GDD and the signal source was adjusted to examine its effect on the peak to peak voltage of the detected signal. It was observed that the peak to peak voltage (Vpp) is higher when the signal source is closer to the GDD than when it is farther away. It should be noted that the Vpp values observed were not net values but rather they were hovering between particular ranges, and we recorded the highest values for each range.

Table 4.4 Effect of distance on 200kHz and 250kHz modulation frequencies

Distance (cm)	Vpp (mV) for 200kHz	Vpp (mV) for 250kHz
1	3.9	3.5
2	3.6	3.2
3	3.52	2.92
4	3.44	2.56
5	3.12	2.48
6	2.8	2.24
7	2.72	2.2
8	2.64	2.16
9	2.56	2.16
10	2.48	2
15	2	1.8

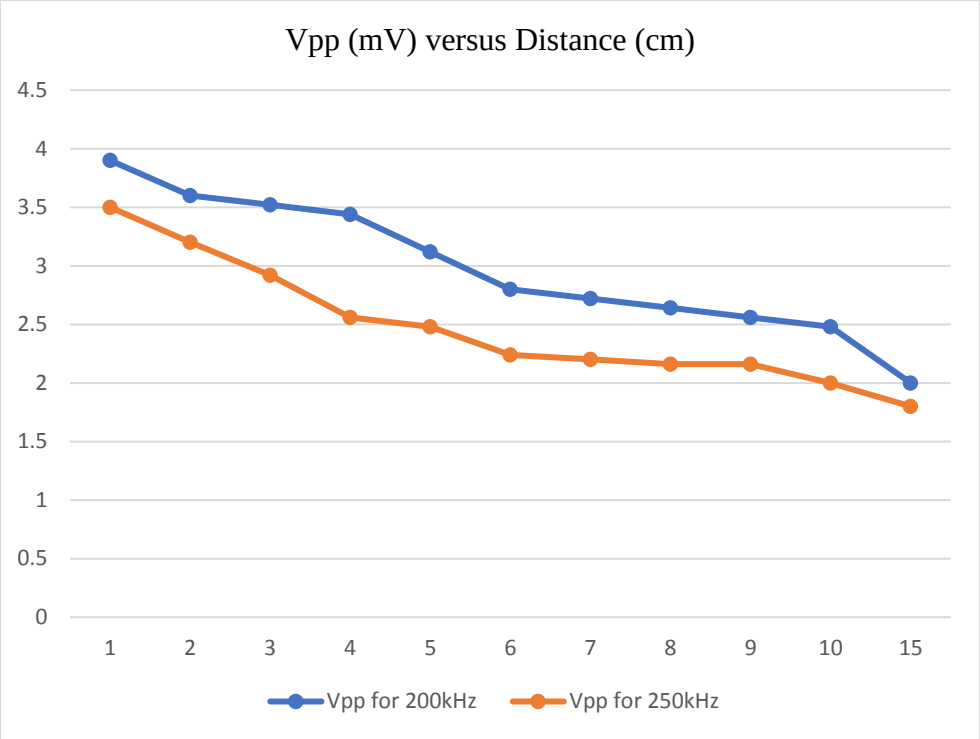


Figure 4.37 Vpp (mV) versus Distance (cm) for microwave

CHAPTER 5

CONCLUSION

The performance of an AC driven GDD while detecting a THz signal of 60GHz modulated at 170kHz as well as a microwave signal of 10.5GHz has been comprehensively studied. Firstly, an in-depth theoretical study of glow discharge physics and a synopsis on microwave and millimeter wave radiations have been given. Moreover, a comprehensive review of research work done on using neon indicator lamps as GDDs for detecting microwave and millimeter wave signals has also been conducted and this was to get a profound insight into the specific objectives of the research which included; biasing the GDD with alternating current (AC), examining the relationship between the modulation frequency and the peak to peak voltage of the received THz signal, analyzing the signal before and after filtering and amplification, analyzing the GDD responsivity with respect to time as well as examining the effect of the distance between the microwave signal source and the GDD.

It has been observed that driving the GDD with alternating voltage solves the problem of GDD burn-out that's associated with DC driven GDDs. Even so, it has been experimentally proved that the GDD responsivity of a DC driven GDD diminishes with time whereby within 10 minutes the responsivity drops from 100mV to 42mV. Furthermore, microwave interaction with an AC driven GDD has also been experimentally examined in that the effect of the distance between the signal source of 10.5GHz and the GDD on the signal peak to peak voltage (Vpp) for peculiar modulation frequencies has been analyzed. The most efficient modulation frequency is found to be 200kHz followed by 250kHz.

5.1 FUTURE WORK

We suggest that further research on AC driven GDDs should be conducted while using tunable RF oscillators to examine the GDD performance over a wide range of frequencies. We also recommend that different types of GDDs should be examined with AC biasing to ascertain the best type for detection applications.

REFERENCES

[1] Abramovich, A., Kopeika, N. S., & Rozban, D. THz Polarization Effects on Detection Responsivity of Glow Discharge Detectors (GDDs). IEEE Sensors Journal, *9*, 10, OCTOBER 2009.

[2] Lei, H., Hongkyu, P., & Xi-Cheng Z. Terahertz Wave Imaging System Based on Glow Discharge Detector. IEEE Journal of Selected Topics in Quantum Electronics, *17*, 1, January/February 2011.

[3] Brown, E. R. A system-level analysis of Schottky diodes for incoherent THz imaging arrays. Solid-State Electron, *48*, 2051-2053, October/November 2004.

[4] Maestrini, A., Ward, J., Gill, J., Javadi, H., Schlecht, E., & Chattopadhyaym, G. A 1.7–1.9 THz local oscillator source. IEEE Microwave Wireless Compon. Lett., *14*, 6, 253–255, June 2004.

[5] Kopeika, N. S. Theory of a fast, sensitive, submillimeter wave glow discharge detector. Int. J. Infrared Milli Waves, *5*, 1333-1348, September 1984.

[6] Reece Roth, J. *Industrial Plasma Engineering, Volume 1: Principles.* Institute of Physics (IOP) Publishing Ltd. 1995.

[7] Glow Discharge. Retrieved from http://webhost.ua.ac.be/plasma/pages/glow-discharge.

[8] Stephanie A. W., Andrew Z., Jerry R., & Sophia G. The Use of DC Glow Discharges as Undergraduate Educational Tools.

[9] Michael A. L., Allan J. L. *Principles of Plasma Discharges and Materials Processing.* John Wiley & Sons, Inc. 1994.

[10] Kunze, H. J. *Introduction to Plasma Spectroscopy*. Springer-Verlag Berlin Heidelberg. 2009.

[11] Asghar, H., Ali, R., & Baig, M. A. Determination of transition probabilities for the 3p→ 3s transition array in neon using laser induced breakdown spectroscopy. Physics of Plasmas, *20*, 12, 123302, 2013.

[12] Mahmood, S., Shaikh, N. M., Kalyar, M. A., Rafiq, M., Piracha, N. K., & Baig, M. A. Measurements of electron density, temperature and photoionization cross sections of the excited states of neon in a discharge plasma. Journal of Quantitative Spectroscopy and Radiative Transfer, *110*, 17, 1840-1850, 2009.

[13] Griem, H. R. *Principles of Plasma Spectroscopy*. Cambridge: Cambridge University Press. 1997.

[14] Gondal, M. A., Maganda, Y. W., Dastageer, M. A., Al Adel, F. F., Naqvi, A. A.,& Qahtan, T. F. Detection of the level of fluoride in the commercially available toothpaste using laser induced breakdown spectroscopy with the marker atomic transition line of neutral fluorine at 731.1 nm. Optics & Laser Technology, 57, 32-38, 2014.

[15] Kopeika, N. S. On the mechanism of glow discharge detection of microwave and millimeter-wave radiation. Proceedings of the IEEE, *63*, 6, 981-982, 1975.

[16] Moisan, M., & Pelletier, J. Individual motion of a charged particle in electric and magnetic fields. Physics of Collisional Plasmas, 101-202, Springer Netherlands, 2012.

[17] Brown, S. C. *Introduction to Electrical Discharges in Gases*. John Wiley & Sons. 1968.

[18] Jackson, J. D. *Classical Electrodynamics*. John Wiley & Sons. 1999.

[19] Vanderlinde, J. *Classical Electromagnetic Theory*. Springer Science+Business Media. 2005.

[20] Zheng, L., Zhao, Q., Liu, S., Xing, X., & Chen, Y. Theoretical and experimental studies of terahertz wave propagation in unmagnetized plasma. Journal of Infrared, Millimeter, and Terahertz Waves, *35*, 2, 187-197, 2014.

[21] Zheng, L., Zhao, Q., Liu, S., Ma, P., Huang, C., Tang, Y., & Luo, X. Theoretical and experimental studies of 35 GHz and 96 GHz electromagnetic wave propagation in plasma. Progress in Electromagnetics Research, *24*, 179-192, 2012.

[22] Kopeika, N. S. Glow discharge detection of long wavelength electromagnetic radiation: Cascade ionization process internal signal gain and temporal and spectral response properties. IEEE Transactions on Plasma Science, *6*, 2, 139-157, 1978.

[23] Farhat, N. H. Optimization of millimeter-wave glow-discharge detectors. Proceedings of the IEEE, *62*, 2, 279-281, 1974.

[24] Kopeika, N. S., Galore, B., Stempler, D., & Heimenrath, Y. Commercial Glow Discharge Tubes as Detectors of X-Band Radiation. IEEE Transactions on Microwave Theory and Techniques, *23*, 10, 843-846, October 1975.

[25] Yaakov M., Oded R. M., & Kopeika, N. S. Very High Sensitivity Heterodyne Detection of X-Band Radiation with Neon Indicator Lamps. IEEE Transactions on Microwave Theory and Techniques, *26*, 1, January 1978.

[26] Kopeika, N. S., Makover, Y., & Schonbach, S. IF Conversion Gain of GLOW Discharge Lamps as X-Band Mixers for High LO Power Levels. IEEE Transactions on Microwave Theory and Techniques, *27*, 3, 227-232, April 1979.

[27] Kopeika, N. S., Even Z. D., & Fishbe, I. Low-Cost Glow Discharge Tube Microwave Frequency Sensor. Proceedings of the IEEE, March 1976.

[28] Kopeika, N. S., & Farhat, N. H. Video Detection of Millimeter Waves with Glow Discharge Tubes: Part I – Physical Description; Part II - Experimental Results. IEEE Transactions on Electron Devices, *22*, 8, August 1975.

[29] Kamil C., Hasan M. B. & Hakan, A. Characterization of a Glow Discharge Detector with Terahertz Time Domain Spectroscopy. IEEE Sensors Journal, *13*, 7, JULY 2013.

[30] Assaf L., Kopeika, N. S. Yitzhak Y., Daniel R., & Amir A. Calibration Method for MMW Imaging Using Inexpensive Miniature Neon Indicator Lamp Detectors. IEEE Sensors Journal, *14*, 5, May 2014.

[31] Daniel R., Avihai, A., Amir A., & Kopeika, N. S. Switching and Fast Operation of Glow Discharge Detector for Millimeter Wave Focal Plane Array Imaging Systems. IEEE Sensors Journal, *15*, 11, November 2015.

[32] Avihai A., Daniel R., Avi K., Amir A., Yitzhak Y., & Kopeika, N. S. Detection and up-conversion of three-dimensional MMW/THz images to the visible. Photon. Res., *4*, 6, December 2016.

[33] Avihai A., Daniel R., Kopeika, N. S., & Amir A. Heterodyne detection at 300 GHz using neon indicator lamp glow discharge detector. Applied Optics, *52*, 17, 10 June 2013.

[34] Hezi J., Kopeika, N. S., Abramovich, A., Akram, A., Levanon, A. & Rozban, D. Heterodyne Detection by Miniature Neon Indicator Lamp Glow Discharge Detectors. IEEE Sensors Journal, *11*, 9, September 2011.

[35] Abramovich, A., Kopeika, N. S., Rozban, D., & Farber, E. Inexpensive detector for terahertz imaging. Applied Optics, *46*, 29, 10 October 2007.

[36] Mehta, A. Introduction to the Electromagnetic Spectrum and Spectroscopy. Retrieved February 24, 2019 from https://pharmaxchange.info/2011/08/introduction-to-the-electromagnetic-spectrum-and-spectroscopy.

[37] Herley. *Microwave Oscillator notes*. General Microwave.

[38] Brown, E. R., Soderstrom, J. R., Parker, C. D., Mahoney, L. J., Molvar, K. M., & McGill, T. C. Oscillations up to 712 GHz in InAs/AlSb resonant-tunneling diodes. *Applied Physics Letters*, *58*, 20, 2291, 1999.

CURRICULUM VITAE

PERSONAL INFORMATION



Name Surname: HUSSEIN SSALI

Nationality: Ugandan

Date of Birth: 25/10/1990

Phone : +905457269335

E-mail : ssalihussein90@gmail.com

EDUCATION

Bachelor's Degree: B.Eng. in Telecommunications Engineering, Kyambogo University, Kampala-Uganda (2011-2015).

Master's Degree: MSc. Electrical and Electronics Engineering, Ankara Yildirim Beyazit University, Ankara-Turkey (2017-2019).

CONFERENCES ATTENDED

3rd International Symposium on Innovative Approaches in Scientific Studies. April 2019, Ankara-Turkey.

PUBLICATIONS

Hussein, S. & Asaf, B. S. Detecting Microwave Signals (X-band) Using Glow Discharge Detectors, SETSCI Conference proceedings, 4(1):306-309, May 2019.

WORK EXPERIENCE

Site Engineer at Huawei Technologies (U) Ltd (Sept 2015 to 31st Dec 2015).

TOPICS OF INTEREST

-Communications engineering -RF and THz technologies and applications


ANKARA YILDIRIM BEYAZIT ÜNİVERSİTESİ